

Unexpectedly different reactions of [(arene)Mn(CO)₃]⁺ cations (arene = trindane, indane, tetralin, or dibenzosuberane) with potassium *t*-butoxide — C-H insertions, haptotropic shifts, dimerization, or elimination¹

Nada Reginato, Laura E. Harrington, Yannick Ortin, and Michael J. McGlinchey

Abstract: [(η^6 -Trindane)Mn(CO)₃][BF₄] (**1**) reacts with *tert*-BuOK in THF in the presence of alkyl halides (CH₂=CHCH₂Br, CH₃I) to yield the corresponding (η^6 -C₁₅H₁₈)Mn(CO)₂X, where X = Br (**3**) or I (**4**). In contrast, **1** and *tert*-BuOK react, in the presence of a donor ligand, to generate (η^5 -C₁₅H₁₅)Mn(CO)₂L, where L = CO (**7**), P(OMe)₃ (**8**), or PPh₃ (**9**), in which the metal has migrated from the central ring onto a peripheral ring that has lost three hydrogens; [(η^6 -indane)Mn(CO)₃][BF₄] behaves similarly. A mechanism is proposed in which the initially formed (η^6 -trindane)Mn(CO)₂CO₂-*tert*-Bu suffers the loss of CO₂ and isobutene to yield the hydride, (η^6 -trindane)Mn(CO)₂H, that in turn undergoes three successive C-H insertions with concomitant loss of two molecules of dihydrogen. In contrast, [(η^6 -tetralin)Mn(CO)₃][PF₆] (**17**) and [(η^6 -dibenzosuberane)Mn(CO)₃][BF₄] (**23**) each suffer deprotonation at a benzylic site. In the first case, the zwitterion formed attacks its progenitor to yield a tetralenyl-substituted (η^5 -cyclohexadienyl)Mn(CO)₃ complex (**21**); however, for the dibenzosuberane complex (**23**) the elimination product (**28**) is stable. X-ray crystal structures are reported for **3**, **4**, **7**, **8**, **23**, **28**, and for the phosphite complexes [(η^6 -trindane)Mn(CO){P(OMe)₃}₂][BF₄] (**15**) and [(η^6 -tetralin)Mn(CO)₂{P(OMe)₃}][PF₆] (**20**).

Key words: arene–manganese, organometallic cations, deprotonations, X-ray crystallography.

Résumé : Le [(η^6 -trindane)Mn(CO)₃][BF₄] (**1**) réagit avec la *tert*-BuOK, dans le THF, en présence d'halogénures d'alkyles (CH₂=CHCH₂Br et le CH₃I) pour conduire à la formation des (η^6 -C₁₅H₁₈)Mn(CO)₂X dans lesquels X = Br (**3**) ou I (**4**). Par opposition, le composé **1** réagit avec la *tert*-BuOK, en présence d'un ligand donneur, pour générer les complexes (η^5 -C₁₅H₁₅)Mn(CO)₂L dans lesquels L = CO (**7**), P(OMe)₃ (**8**) ou PPh₃ (**9**) alors que le métal a migré du noyau central vers un noyau périphérique avec perte de trois atomes d'hydrogène; Le [(η^6 -indane)Mn(CO)₃][BF₄] se comporte de la même manière. On propose un mécanisme dans lequel l'entité (η^6 -trindane)Mn(CO)₂CO₂-*tert*-Bu subit une perte de CO₂ et d'isobutène pour fournir l'hydruire (η^6 -trindane)Mn(CO)₂H qui subit à son tour trois insertions successives de C-H avec la perte concomitante de deux molécules de dihydrogène. Par ailleurs, le [(η^6 -tétraline)Mn(CO)₃][PF₆] (**17**) et le [(η^6 -dibenzosubérane)Mn(CO)₃][BF₄] (**23**) subissent chacun une déprotonation au niveau du site benzylique. Dans le premier cas, le zwitterion qui est formé attaque son progéniteur pour conduire à la formation d'un complexe (η^5 -cyclohexadiényl)Mn(CO)₃ portant un substituant tétralényle (**21**); toutefois, pour le complexe avec le dibenzosubérane (**23**), le produit d'élimination (**28**) est stable. Faisant appel à la diffraction des rayons X, on a déterminé et on décrit les structures cristallines des composés **3**, **4**, **7**, **8**, **23** et **28** ainsi que celles des complexes de phosphite, [(η^6 -trindane)Mn(CO){P(OMe)₃}₂][BF₄] (**15**) et [(η^6 -tétraline)Mn(CO)₂{P(OMe)₃}][BF₆] (**20**),

Mots-clés : arene–manganèse, cations organométalliques, déprotonations, cristallographie par diffraction des rayons X.

[Traduit par la Rédaction]

Received 31 March 2008. Accepted 14 May 2008. Published on the NRC Research Press Web site at canjchem.nrc.ca on 3 October 2008.

This article is dedicated to Professor Richard Puddephatt, an outstanding chemist, an inspiring teacher, and a valued friend.

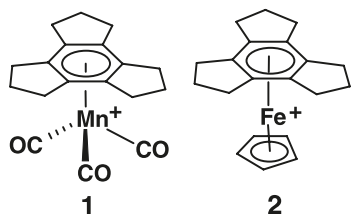
N. Reginato and L.E. Harrington. Department of Chemistry, McMaster University, Hamilton, ON L8S 4M1, Canada.
Y. Ortin and M.J. McGlinchey.² School of Chemistry and Chemical Biology, University College Dublin, Belfield, Dublin 4, Ireland.

¹This article is part of a Special Issue dedicated to Professor Richard J. Puddephatt.

²Corresponding author (e-mail: michael.mcglinchey@ucd.ie).

Introduction

As part of a program directed towards an organometallic route to sumanene (1), we began to develop the organometallic chemistry of tri(cyclopentano)benzene (trindane) (2, 3), a tetracyclic substructure of the target molecule. To this end, we chose to attempt the alkylation of all six *exo*-benzylic positions of $(\eta^6\text{-trindane})\text{ML}_n$ using the now classic Astruc methodology (4). Since Eyman and co-workers (5) have already shown that [(hexamethylbenzene) $\text{Mn}(\text{CO})_3$]⁺ readily undergoes abstraction of a benzylic proton to yield the corresponding cyclohexadienyl system that reacts with electrophiles to functionalize the benzylic site (5), we decided to study the reactions of $[(\eta^6\text{-trindane})\text{Mn}(\text{CO})_3][\text{BF}_4]$ (**1**) and $[(\eta^6\text{-trindane})\text{Fe}(\text{C}_5\text{H}_5)][\text{PF}_6]$ (**2**) with potassium *tert*-butoxide, and subsequently with alkyl halides. However, as reported in a preliminary communication (6), the reactions of **1** led to unexpected rearrangement products. We now describe these studies more fully, and also report how the reactions have been extended to the analogous $[(\eta^6\text{-arene})\text{Mn}(\text{CO})_3]^+$ systems, whereby the five-membered rings in trindane or indane have been replaced by six- and seven-membered rings in tetralin and dibenzosuberane, respectively.



Results and discussion

The activation of benzylic sites by incorporation of a π -complexed organometallic moiety is a well-established phenomenon, and has been attributed to a combination of the electron-withdrawing effect of the metal and the resonance stabilization of the conjugate base (7). Typically, molecules of the type $(\eta^6\text{-arene})\text{ML}_n$, where ML_n is $\text{Cr}(\text{CO})_3$, $\text{Mn}(\text{CO})_3^+$, or $\text{Fe}(\text{C}_5\text{H}_5)^+$, undergo ready deprotonation at benzylic positions; subsequent treatment with alkyl halides leads to attack at the benzylic site. Particularly elegant examples are provided by Jaouen et al.'s (8) specific functionalization at the $\beta\beta$ position in (3-methoxyestradiol)[$\alpha\text{-Cr}(\text{CO})_3$], and by Astruc's (9) systematic construction of organometallic dendrimers. Another very ingenious application that takes advantage of the steric blocking of one face of the arene by a metal tripod is the preparation of an artificial receptor, whereby trindane was benzylated at the three *exo*-wingtip positions (10).

Reactions of $[(\eta^6\text{-trindane})\text{Fe}(\text{C}_5\text{H}_5)][\text{PF}_6]$

In light of these precedents, $[(\eta^6\text{-trindane})\text{Fe}(\text{C}_5\text{H}_5)][\text{PF}_6]$ (**2**) and *tert*-BuOK were mixed as dry solids and then treated with excess allyl bromide (or methyl iodide) in THF in the hope that all six *exo*-benzylic sites would be alkylated. In a previous study (2), we had noted that the corresponding reaction of **2** and *tert*-BuOK in the presence of DMSO-*d*₆ yielded dodeca-deuterated **2** as the major product; that is, all twelve benzylic positions, both *exo* and *endo*, had undergone exchange. Interestingly, use of either allyl bromide or methyl

iodide again led to extensive multiple alkylation, and mass spectrometric data indicated the incorporation of at least ten, and possibly twelve, allyl or methyl substituents. After many attempts to obtain a sample of the polymethylated complex appropriate for an X-ray study, data sets were acquired on several crystals of rather poor quality, but disorder problems have so far prevented the satisfactory resolution of these structures.

Reactions of $[(\eta^6\text{-trindane})\text{Mn}(\text{CO})_3][\text{BF}_4]$

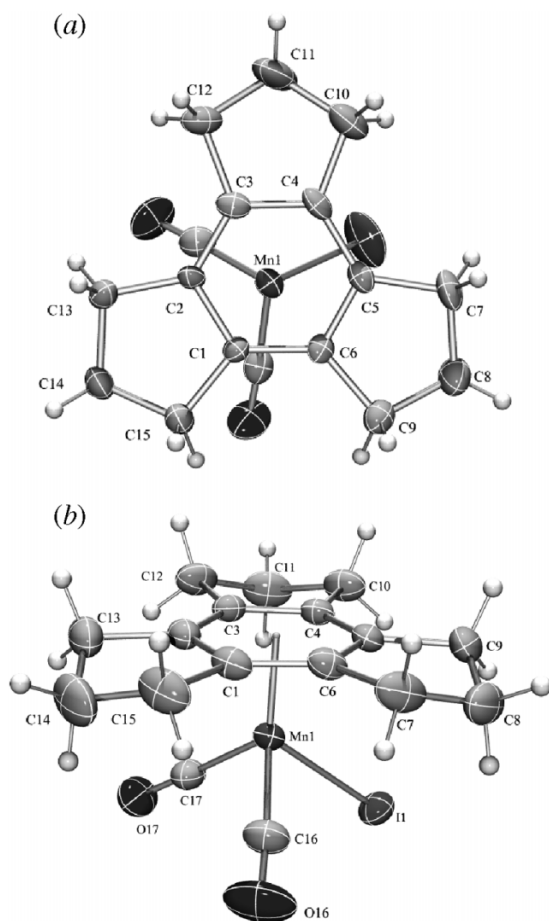
Since an $\text{M}(\text{CO})_3$ moiety ($\text{M} = \text{Cr}, \text{Mn}$) has been shown to generate a larger cone angle than an $\text{Fe}(\text{C}_5\text{H}_5)$ fragment (11), the tripodal group $\text{Mn}(\text{CO})_3^+$ was selected as an activating agent, not only to enhance the acidity at the benzylic positions but in addition to act as a stereodirecting group by blocking one π -face of the arene ligand. Consequently, our focus switched to the manganese cation, **1**, which, when mixed with *tert*-BuOK as dry solids, and then treated with excess allyl bromide in THF furnished after chromatographic separation a deep red crystalline material whose NMR, mass, and IR spectra indicated it to be $(\eta^6\text{-trindane})\text{Mn}(\text{CO})_2\text{Br}$ (**3**). The analogous reaction of **1**, *tert*-BuOK, and methyl iodide gave the corresponding $(\eta^6\text{-trindane})\text{Mn}(\text{CO})_2\text{I}$ (**4**).

The X-ray crystal structures of **3** and **4** appear in Figs. 1a and 1b, respectively, and are reminiscent of the geometry previously reported for $(\eta^6\text{-C}_6\text{Me}_6)\text{Mn}(\text{CO})_2\text{Cl}$ whereby the tripod is staggered relative to the alkyl substituents (12). Moreover, the cyclopentene rings in **3** (and **4**) adopt envelope conformations such that the "wingtip" methylene groups are folded endo with respect to the plane of the central six-membered ring, as was previously found in both $(\eta^6\text{-trindane})\text{Cr}(\text{CO})_3$ and $[(\eta^6\text{-trindane})\text{RuCl}_2\{\text{P}(\text{OMe})_3\}]$ (2, 3). The structures of **3** and **4** may also be compared with the known complexes $[\text{tri}(\text{cyclohexano})\text{benzene}]\text{ML}_n$, where $\text{ML}_n = \text{Cr}(\text{CO})_3$ or $\text{Mn}(\text{CO})_3^+$, whereby the $\text{M}(\text{CO})_3$ unit displays the typical staggered orientation and the peripheral rings exhibit the "half-boat" conformation (13).

Another structural feature of interest for compounds **3** and **4** is that, in each case, the central ring is slightly folded such that the arene carbons C(1) and C(2), trans to the halogen atom, are slightly closer to the manganese atom than are the other four carbons [i.e., C(3), C(4), C(5), C(6)]. Whether this folding is attributable to packing effects, or to the weaker trans influence of the halide, is not clear; however, it parallels the folding found in $(\eta^6\text{-C}_6\text{Me}_6)\text{Mn}(\text{CO})_2\text{Cl}$. The manganese atoms in **3** and **4** are located 1.677 and 1.678 Å, respectively, below the centroid of the six-membered ring, slightly closer than is found in $(\eta^6\text{-C}_6\text{Me}_6)\text{Mn}(\text{CO})_2\text{Cl}$ (1.706(3) Å) (12). The Mn–CO bond lengths are normal (1.781(8)–1.802(10) Å), the Mn–C–O angles are slightly less than 180°, and the Mn–ring–carbon distances range from 2.133(7) to 2.230(4) Å.

As expected, the carbonyl IR stretching frequencies in the series $(\eta^6\text{-trindane})\text{Mn}(\text{CO})_2\text{X}$ decrease as a result of the transformation from a cationic to a neutral species: X = Cl (1980, 1931 cm^{-1}), X = Br (1971, 1927 cm^{-1}), X = I (1973, 1926 cm^{-1}). The starting material, $[(\eta^6\text{-trindane})\text{Mn}(\text{CO})_3][\text{BF}_4]$ (**1**) exhibits carbonyl stretches at 2056 and 1997 cm^{-1} . These data are similar to the ν_{CO} values previously reported for $(\eta^6\text{-C}_6\text{Me}_6)\text{Mn}(\text{CO})_2\text{X}$ complexes: 1972, 1920 cm^{-1} ; 1971,

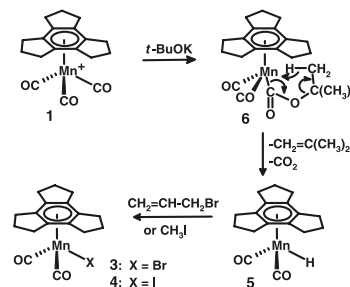
Fig. 1. (a) The molecular structure of $(\eta^6\text{-trindane})\text{Mn}(\text{CO})_2\text{Br}$ (**3**) showing the staggered orientation of the tripodal $\text{Mn}(\text{CO})_2\text{Br}$ moiety. (b) The molecular structure of $(\eta^6\text{-trindane})\text{Mn}(\text{CO})_2\text{I}$ (**4**) illustrating the envelope conformation of the peripheral rings. Thermal ellipsoids are shown at the 30% probability level.



1921 cm^{-1} ; and 1968, 1920 cm^{-1} ; where X = Cl, Br, and I, respectively (12).

Since replacement of a carbonyl by a phosphine or a halide in $[(\eta^6\text{-C}_6\text{Me}_6)\text{Mn}(\text{CO})_3]^+$ normally requires either photolysis or use of Me_3NO (14, 15), it was somewhat surprising that the formation of the $(\eta^6\text{-trindane})\text{Mn}(\text{CO})_2\text{X}$ species, **3** and **4**, should have occurred so readily. Moreover, because $(\eta^6\text{-C}_6\text{Me}_6)\text{Mn}(\text{CO})_2\text{H}$ is known to yield $(\eta^6\text{-C}_6\text{Me}_6)\text{Mn}(\text{CO})_2\text{Cl}$ in the presence of CCl_4 or CHCl_3 (but not CH_2Cl_2) (12), one is tempted to invoke the intermediacy of $(\eta^6\text{-trindane})\text{Mn}(\text{CO})_2\text{H}$ (**5**). Eyman and co-workers (16) have shown that $(\eta^6\text{-C}_6\text{Me}_6)\text{Mn}(\text{CO})_2\text{I}$ reacts with *tert*-butyllithium to yield thermally stable $(\eta^6\text{-C}_6\text{Me}_6)\text{Mn}(\text{CO})_2\text{H}$, apparently via loss of isobutene from the presumed *tert*-butyl intermediate. Furthermore, as the cationic complexes $[(\eta^6\text{-arene})\text{Mn}(\text{CO})_3]^+$, (arene = C_6H_6 or C_6Me_6), are known to react with methoxide in methanol to yield the rather unstable esters, $(\eta^6\text{-arene})\text{Mn}(\text{CO})_2\text{CO}_2\text{Me}$ (17), one might propose that a reaction between **1** and *tert*-BuOK could generate the *tert*-butyl ester (**6**) that readily eliminates both isobutene and carbon dioxide via a very favorable six-membered transition state to produce **5**, as depicted in Scheme 1. Interestingly, treatment of **1** with *tert*-BuOK in CH_2Cl_2 gave $(\eta^6\text{-trindane})\text{Mn}(\text{CO})_2\text{Cl}$, suggesting that **5** is

Scheme 1. Proposed mechanism of formation of **3** and **4**.



more reactive than $(\text{C}_6\text{Me}_6)\text{Mn}(\text{CO})_2\text{H}$ towards alkyl halides.

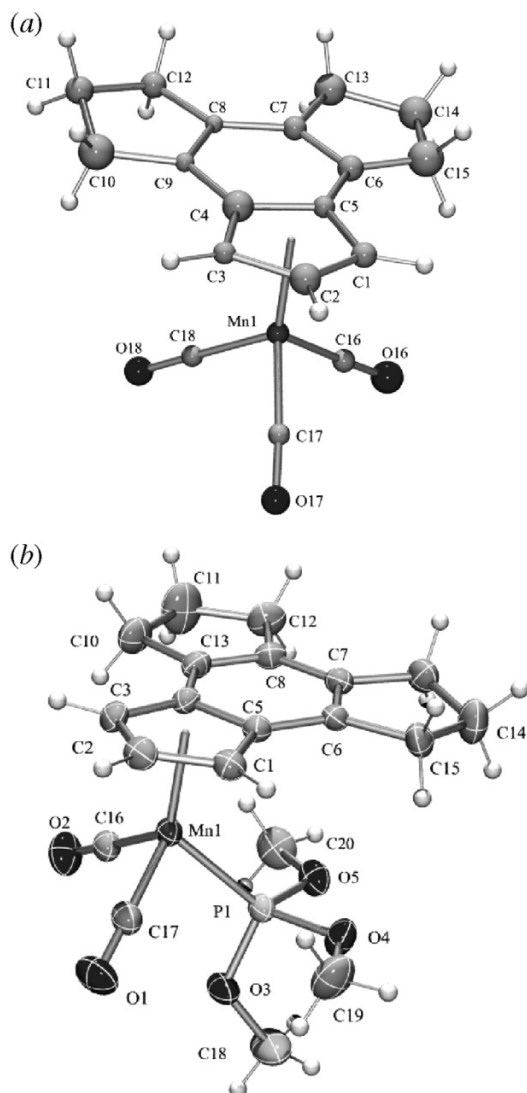
Although it is well established that $(\text{C}_6\text{Me}_6)\text{Mn}(\text{CO})_2\text{H}$ can be prepared by treatment of $(\text{C}_6\text{Me}_6)\text{Mn}(\text{CO})_2\text{Br}$ with $[\text{Bu}_4\text{N}][\text{BH}_4]$ (12), numerous attempts to synthesize $(\eta^6\text{-trindane})\text{Mn}(\text{CO})_2\text{H}$ from the corresponding bromide **3** by this route, or to detect the hydride signal by NMR at low temperature, were unsuccessful. Consequently, we chose to try to intercept the purported hydride **5**, either as $(\text{trindane})\text{Mn}(\text{CO})(\text{PR}_3)\text{H}$, or as the formyl complex $(\text{trindane})\text{Mn}(\text{CO})(\text{CHO})(\text{PR}_3)$, in the absence of RBr.

When the cation **1** and *tert*-BuOK were treated with trimethyl phosphite in THF and allowed to stir at 40 °C for 20 h, to our surprise, the two products isolated after chromatographic separation, were yellow crystalline materials **7** and **8** whose ^1H and ^{13}C NMR spectra indicated that the three-fold symmetry of the trindane ligand had been broken. The mass spectra of **7** and **8** exhibited parent peaks at $m/z = 334$ and 430, respectively, indicating a molecular formula of $(\text{C}_{15}\text{H}_{15})\text{Mn}(\text{CO})_2\text{L}$, where L = CO for **7**, and L = $\text{P}(\text{OMe})_3$ for **8**. Both products were definitively characterized by X-ray crystallography as η^5 -indenyl complexes in which the manganese has migrated from the central arene onto a five-membered ring that has evidently lost three hydrogens. The analogous complex (**9**), where L = PPh_3 , is also accessible in this manner. Likewise, the corresponding reactions of $[(\eta^6\text{-indane})\text{Mn}(\text{CO})_3][\text{BF}_4]$ (**10**) and *tert*-BuOK yield the known complexes $(\eta^5\text{-indenyl})\text{Mn}(\text{CO})_2\text{L}$, where L = $\text{P}(\text{OMe})_3$ or PPh_3 (18). The IR spectra of **7** (ν_{CO} absorptions at 2016 and 1934 cm^{-1}) and **8** (ν_{CO} at 1944 and 1876 cm^{-1}) each exhibit two carbonyl bands, and are in accord with those of the closely analogous systems $(\eta^5\text{-C}_5\text{H}_5)\text{Mn}(\text{CO})_3$ (ν_{CO} at 2025 and 1938 cm^{-1}) and $(\eta^5\text{-C}_5\text{H}_5)\text{Mn}(\text{CO})_2[\text{P}(\text{OMe})_3]$ (ν_{CO} at 1948 and 1884 cm^{-1}).

The structures of the rearranged molecules **7** and **8** are shown in Figs. 2a and 2b, respectively, and reveal in each case a “piano stool” structure with the $\text{Mn}(\text{CO})_2\text{L}$ tripod coordinated in an η^5 -fashion to a peripheral five-membered ring. The manganese atoms in **7** and **8** lie 1.824 and 1.797 Å, respectively, below the centroid of the five-membered ring. The Mn-to-cyclopentadienyl-carbon distances range from 2.114(2) to 2.235(2) Å, and are comparable to those reported for $(\eta^5\text{-cyclopenta}[def]\text{phenanthrenyl})\text{Mn}(\text{CO})_3$ (19).

In Scheme 2, a mechanistic rationale to account for these novel products is offered. We suggest that in the absence of an alkyl halide, the initially generated $(\text{trindane})\text{Mn}(\text{CO})_2\text{H}$ (**5**) undergoes a hydrogen migration (presumably via an agostic interaction) from an *endo*-benzyl site onto the metal thus producing the cyclohexadienyl complex (**11**) that in turn

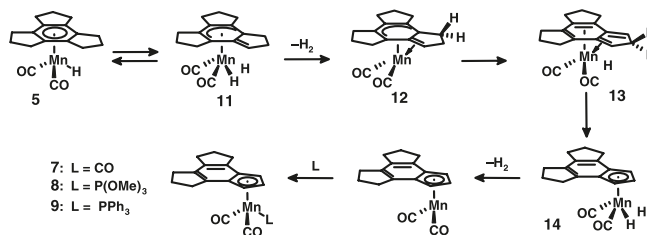
Fig. 2. (a) Molecular structure of $(C_{15}H_{15})Mn(CO)_3$ (**7**). (b) Molecular structure of $(C_{15}H_{15})Mn(CO)_2[P(OMe)_3]$ (**8**). Thermal ellipsoids are shown at the 30% probability level.



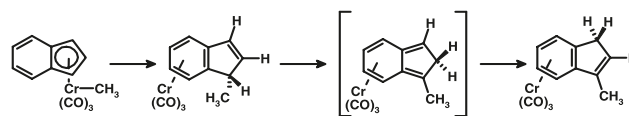
loses dihydrogen to give **12**. A second *endo*-benzyl hydrogen migration to yield the isoindene framework (**13**) is followed by the final hydrogen migration producing **14**. Loss of dihydrogen and incorporation of either a carbonyl or a phosphite ligand would give the observed products **7** or **8**, respectively.

In seeking a precedent for the proposal outlined above, we note the report by Crabtree and Parnell (20) wherein $[(\eta^6\text{-indane})Ir(PPh_3)_2]^+$ undergoes dehydrogenation and an η^6 -to- η^5 haptotropic shift at 80 °C to furnish $[(\eta^5\text{-indenyl})Ir(PPh_3)_2(H)]^+$. Moreover, Ustynyuk and co-workers (21) have shown that $(\eta^5\text{-indenyl})Cr(CO)_3Me$ undergoes a “ricochet reaction” in which the methyl is delivered onto the five-membered ring and the tricarbonylchromium fragment migrates to the six-membered ring, as depicted in Scheme 3. Density functional theory calculations by these workers indicate that the reaction proceeds through an isoindene structure in which the chromium is bonded to the diene portion of the six-membered ring and one double bond of the

Scheme 2. Proposed mechanism of formation of **7**, **8**, and **9**.



Scheme 3. “Ricochet” inter-ring haptotropic rearrangement.



cyclopentadiene ring and provide some justification for the structures **12** and **13** proposed in Scheme 2.

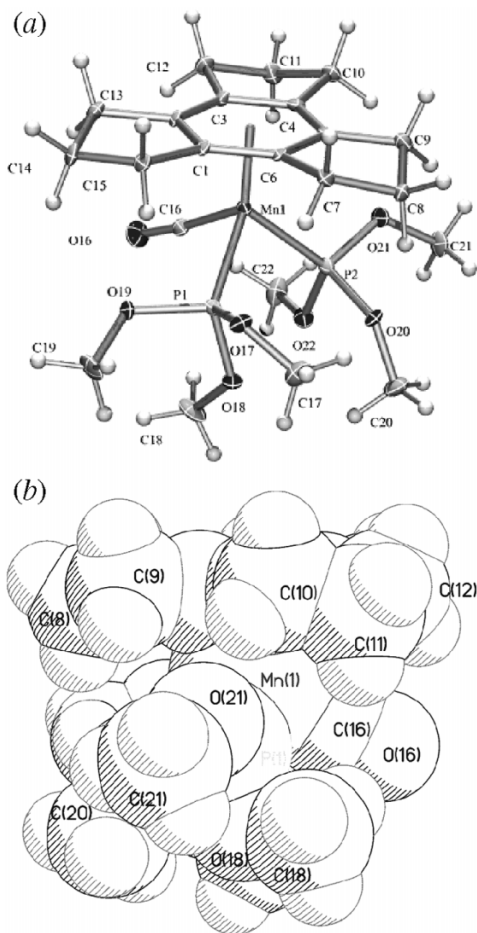
Other (trindane) ML_3 complexes ($M = Mn, Re$)

With the aim of selectively deprotonating only the *exo*-benzylic positions of trindane, we chose to replace one or more of the carbonyl ligands in **1** with somewhat more sterically demanding phosphite substituents, even though such an approach could diminish the acidic character of the benzylic sites. Thus, treatment of $[(\eta^6\text{-trindane})Mn(CO)_3][BF_4]$ (**1**) with trimethyl phosphite and trimethylamine N-oxide furnished a yellow crystalline solid that was characterized spectroscopically and by X-ray crystallography as $[(\eta^6\text{-trindane})Mn(CO)\{P(OMe)_3\}_2][BF_4]$ (**15**). The IR spectrum displayed a single carbonyl stretch at 1911 cm^{-1} , similar to that previously reported for $[(\eta^6\text{-C}_6\text{Me}_6)Mn(CO)\{P(OMe)_3\}_2][PF_6]$ (**14**). Figure 3a depicts the cationic portion of **15**, which has the conventional piano stool structure typical of half-sandwich complexes; the carbonyl and the two trimethyl phosphite ligands adopt a staggered conformation relative to the carbon atoms of the arene ring, and the manganese atom is located 1.724 Å below the centroid of the arene. The Mn–C (arene) bond lengths range from 2.194(4) to 2.237(3) Å, the Mn–CO and two Mn–P distances are 1.772(4), 2.1996(12), and 2.2174(14) Å, respectively, and the Mn–C–O angle is reduced to $173.9(4)^\circ$. As far as we are aware, the only other (arene)manganese-bis-phosphite complex to have been crystallographically characterized is $[(\eta^6\text{-toluene})Mn(CO)\{P(OEt)_3\}_2][PF_6]$ (**22**); the bis-chelated di-tertiary phosphine, $[(\eta^6\text{-C}_6\text{H}_6)Mn(CO)\{\eta^2\text{-PPh}_2(\text{CH}_2)_3\text{PPh}_2\}][PF_6]\cdot 2\text{CH}_3\text{CN}$ and $(\eta^5\text{-C}_6\text{Me}_6\text{H})Mn(CO)[P(OMe)_3]_2$ have also been reported (23, 24).

Figure 3b shows a space-filling view of the degree of crowding on the *endo* side of the complexed trindane ligand, thus restricting access to that face. However, because of the rather poor yield (11%) of **15**, deprotonation or other further reactions of this system were not investigated. This low yield follows the trend observed for analogous compounds such as $[(\eta^6\text{-toluene})Mn(CO)\{P(OR)_3\}_2][PF_6]$ where R is Me or Et (22). Likewise, treatment of $[(\eta^6\text{-toluene})Mn(CO)_3][PF_6]$ with Me_3NO and PPh_3 failed to bring about substitution of the carbonyl groups by triphenylphosphine (24).

In the hope that the hydride $(\eta^6\text{-trindane})Re(CO)_2H$ might show enhanced stability relative to its manganese counter-

Fig. 3. (a) Molecular structure of the cation $[(\eta^6\text{-trindane})\text{Mn}(\text{CO})\{\text{P}(\text{OMe})_3\}_2]^+$ (**15**). Thermal ellipsoids are shown at the 30% probability level. (b) Space-filling view of **15** accentuating the degree of crowding induced by the tripodal fragment.

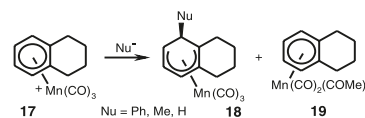


part **5**, it was deemed worthwhile to attempt the synthesis of the analogous $[(\eta^6\text{-trindane})\text{Re}(\text{CO})_3]^+$ cation (**16**). Indeed, **16** can be prepared from $\text{BrRe}(\text{CO})_5$, AlCl_3 , and trindane, but the yield, as is sometimes the case with arene–rhenium complexes (**14**), is very poor (2%). Nevertheless, the $[(\eta^6\text{-trindane})\text{Re}(\text{CO})_3]^+$ cation was readily characterized by IR (ν_{CO} at 2058 and 1966 cm^{-1}) and by electrospray mass spectrometry, which gave rise to distinctive molecular ion peaks at m/z 467 and 469 that exhibited the 37:63 isotopic abundance ratio diagnostic for the presence of ^{185}Re and ^{187}Re . Moreover, the ^1H NMR spectrum exhibited the four chemical environments characteristic of trindane metal carbonyl complexes.

Reactions of $[(\eta^6\text{-tetralin})\text{Mn}(\text{CO})_3][\text{PF}_6]$

To probe the generality of the reaction leading to formation of a hydride intermediate, as in $(\eta^6\text{-trindane})\text{Mn}(\text{CO})_2\text{H}$, and the possibility of dehydrogenation concomitant with a haptotropic shift, the corresponding six-membered tetrahydronaphthalene (tetralin) system was synthesized and treated with potassium *tert*-butoxide and trimethyl phosphite. Following the literature precedent (25), tetralin was treated with bromo(pentacarbonyl)manganese in the presence of aluminum trichloride; subsequent anion ex-

Scheme 4. Reactions of $[(\eta^6\text{-tetralin})\text{Mn}(\text{CO})_3]^+$ (**17**) with nucleophiles.



change furnished $[(\eta^6\text{-tetralin})\text{Mn}(\text{CO})_3][\text{PF}_6]$ (**17**) in 80% yield. We are aware of only one report on the reactivity of the cation **17**, whereby Lee and co-workers (25) found that nucleophilic addition afforded adducts at the α -position, as in **18**, except when treated with MeMgBr in THF at 0 $^\circ\text{C}$, which also yielded the acyl compound **19** (Scheme 4). Related studies by Sweigart and co-workers (26) on hormonal steroidal systems bearing a $[\text{Mn}(\text{CO})_3]^+$ moiety on the aromatic A ring likewise underwent exo addition at C-1 when treated with a range of nucleophiles.

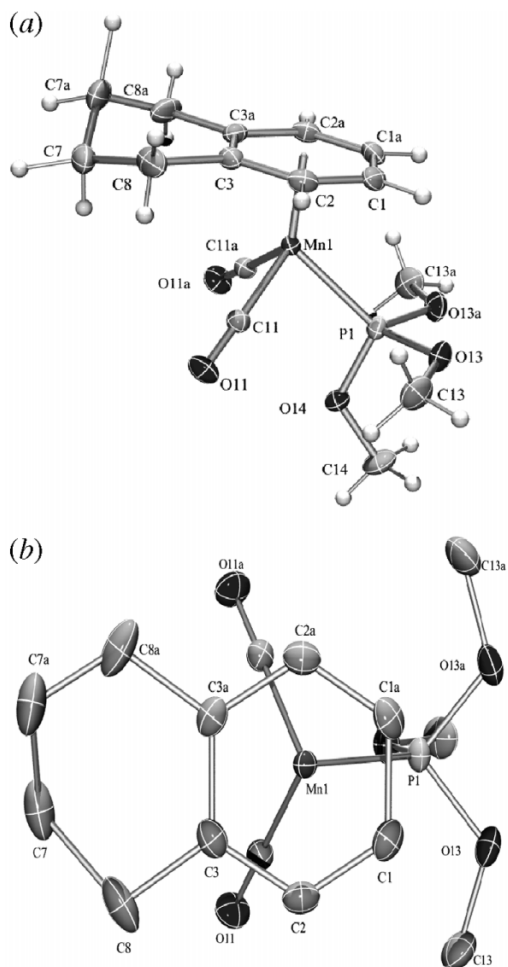
The reaction of $[(\eta^6\text{-tetralin})\text{Mn}(\text{CO})_3][\text{PF}_6]$ (**17**) with *tert*-BuOK and $\text{P}(\text{OMe})_3$ in THF gave, even after repeated chromatographic separations, multiple products each in such low yield as to preclude definitive identification. As a result of the complexity of the reaction, it was decided to investigate the effects of each reagent separately to help clarify their roles in the overall reaction. When trimethyl phosphite in THF was added to $[(\eta^6\text{-tetralin})\text{Mn}(\text{CO})_3][\text{PF}_6]$ in the dark, no change was observed, as monitored by in situ IR spectroscopy. However, when exposed to sunlight, the reaction yielded a yellow crystalline solid that was identified by ^1H , ^{13}C , and ^{31}P NMR and mass spectrometry as $[(\eta^6\text{-tetralin})\text{Mn}(\text{CO})_2\{\text{P}(\text{OMe})_3\}][\text{PF}_6]$ (**20**); the assignment was verified by means of a single crystal X-ray diffraction study. The molecule exhibited carbonyl IR stretches at 2008 and 1961 cm^{-1} , and ^{31}P NMR resonances for each of the phosphorus environments, i.e., for the trimethyl phosphite ligand and the hexafluorophosphate anion.

As shown in Figs. 4a and 4b, the tripodal $[\text{Mn}(\text{CO})_2\{\text{P}(\text{OMe})_3\}]$ unit lies in an essentially staggered orientation, typical of such polycyclic manganese complexes (26). The cyclohexene ring adopts a twisted half-chair conformation, with one of the homobenzylic ring carbon atoms lying below, and the other lying above, the molecular plane defined by the arene ring, which is itself planar. The manganese atom is located 1.679 Å below the plane of the arene ring, and the Mn–C(arene) distances range from 2.179(2) to 2.207(2) Å. The hexafluorophosphate anion was disordered, and two orientations were found.

X-ray crystal structures of related systems in which the tetralin fragment is bound to a $\text{Cr}(\text{CO})_3$ moiety have been reported by Schmalz and co-workers (27). Moreover, these workers investigated the regioselectivity of the deprotonation/alkylation process. Their data revealed that, in the case of two competing exo hydrogen atoms having comparable steric environments, it is not necessarily the *exo*-benzylic hydrogen atom that adopts a pseudoaxial position that is preferentially abstracted. It was concluded that the conformation of the chromium tricarbonyl tripod may influence the regioselectivity of benzylic deprotonation in chiral (arene) $\text{Cr}(\text{CO})_3$ complexes (27), as had been suggested previously (28).

Treatment of $[(\eta^6\text{-tetralin})\text{Mn}(\text{CO})_3][\text{PF}_6]$ (**17**) with potassium *tert*-butoxide in THF afforded a yellow-orange oil that,

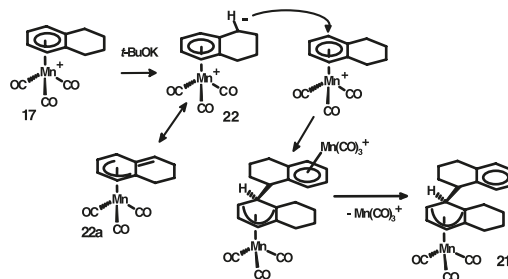
Fig. 4. (a) Molecular structure of the cation in $[(\eta^6\text{-tetralin})\text{Mn}(\text{CO})_2\{\text{P}(\text{OMe})_3\}][\text{PF}_6]$ (**20**); (b) Bird's eye view of **20** illustrates the staggered orientation of the tripodal manganese fragment. Thermal ellipsoids are shown at the 30% probability level.



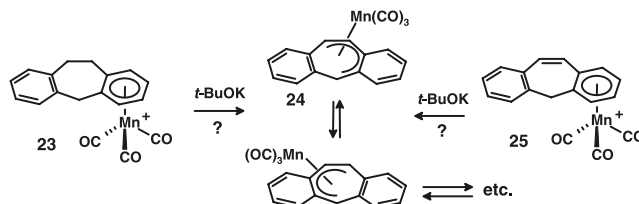
despite repeated efforts, did not yield a crystalline product. Nevertheless, the mass spectrometric and IR data provide strong evidence that the product may be assigned as the tetralenyl-substituted cyclohexadienyl manganese complex **21**. Carbonyl IR absorptions at 2007 and 1927 cm^{-1} (neat) are indicative of a (cyclohexadienyl) $\text{Mn}(\text{CO})_3$ system. For example, nucleophilic attack on $[(\text{tetralin})\text{Mn}(\text{CO})_3]^+$ by hydride, methyl, or phenyl gave the 4-exo-substituted compounds (**18**) that exhibited ν_{CO} peaks (in NaCl) at 2000/1910 cm^{-1} , 2000/1920 cm^{-1} , and 2004/1916 cm^{-1} , respectively, (**25**). Chemical ionization data for **21** revealed an $[\text{M} + \text{H}]^+$ peak at m/z 403, followed by loss of 131 corresponding to $\text{C}_{10}\text{H}_{11}$. Subsequent fragmentation revealed the presence of a tricarbonylmanganese moiety. Because of considerable peak overlap, the ^1H and ^{13}C NMR spectra of **21** have not yet been fully assigned unequivocally, however, efforts to grow X-ray quality crystals are continuing.

A straightforward mechanistic proposal to account for the formation of **21** is depicted in Scheme 5. Deprotonation of $[(\eta^6\text{-tetralin})\text{Mn}(\text{CO})_3][\text{PF}_6]$ by *tert*-BuOK to yield the zwitterionic species **22** (perhaps better represented by the η^5 structure **22a**) can be followed by nucleophilic attack on **17**; subsequent loss of the $[\text{Mn}(\text{CO})_3]^+$ moiety leads directly to **21**.

Scheme 5. Proposed mechanism for the formation of **21**.



Scheme 6. Possible rearrangement reactions of **23** and **25**.

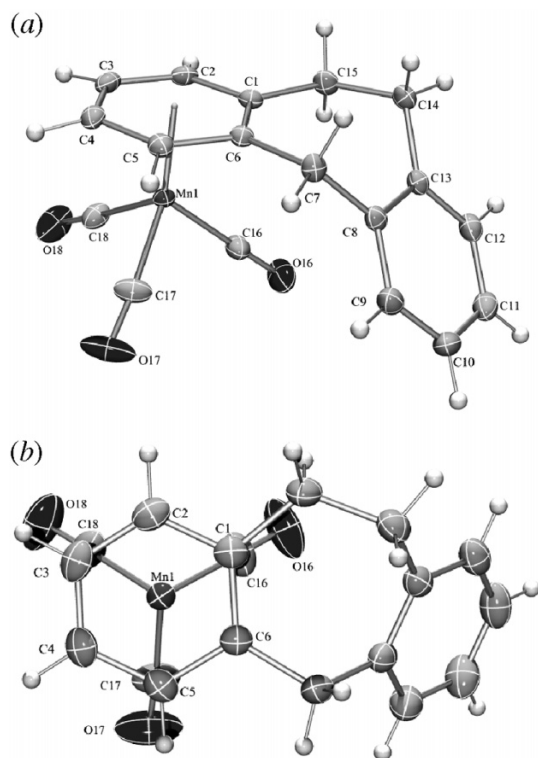


Reactions of $[(\eta^6\text{-dibenzosuberane})\text{Mn}(\text{CO})_3][\text{BF}_4]$

In light of the previously described reactions of the cations $[(\eta^6\text{-trindane})\text{Mn}(\text{CO})_3]^+$ (**1**) and $[(\eta^6\text{-indane})\text{Mn}(\text{CO})_3]^+$ (**10**) with *tert*-BuOK and $\text{P}(\text{OMe})_3$, whereby dehydrogenation of a five-membered ring and concomitant haptotropic shifts yield η^5 complexes, we chose to extend this study to include systems in which the manganese-complexed arene ring was joined to a seven-membered ring. If the reaction of $[(\eta^6\text{-dibenzosuberane})\text{Mn}(\text{CO})_3][\text{BF}_4]$, **23**, were to proceed in a manner analogous to that of the trindane system, **1**, then one might anticipate loss of three hydrogen atoms from the central ring and formation of a $(\eta^5\text{-dibenzocycloheptatrienyl})\text{Mn}(\text{CO})_3$ complex, such as **24**, which might exhibit a fluxional process (Scheme 6) that would equilibrate the two six-membered rings. It has previously been reported that deprotonation of $(\eta^6\text{-benzocycloheptatriene})\text{Cr}(\text{CO})_3$ leads to an η^6 -to- η^5 haptotropic shift such that the metal, which was originally located on the arene ring, is now bonded in an η^5 fashion in the seven-membered ring (**29**). If an analogous migration were to occur upon deprotonation of $[(\eta^6\text{-dibenzosuberane})\text{Mn}(\text{CO})_3]^+$, **25**, the centrally bonded manganese in **24** would presumably exhibit fluxionality, as does $(\eta^5\text{-C}_7\text{H}_7)\text{Mn}(\text{CO})_3$ (**30**).

To this end, $[(\eta^6\text{-dibenzosuberane})\text{Mn}(\text{CO})_3][\text{BF}_4]$ (**23**) was prepared by reaction of dibenzosuberane, bromopentacarbonylmanganese, and silver tetrafluoroborate in dichloromethane and was characterized spectroscopically and by X-ray crystallography. Electrospray mass spectrometry revealed a parent ion at m/z 333, with fragmentation peaks at 277 and 249 corresponding to loss of two and three carbonyls, respectively. The carbonyl IR stretching vibrations peaks at 2065 and 2014 cm^{-1} are typical of arene-manganese tricarbonyl cations, and the ^1H and ^{13}C NMR spectra reveal the presence of one coordinated and one uncoordinated arene ring, and three methylene groups; in each case the methylene protons are rendered nonequivalent by the presence of the metal tripod on one face of the molecule. The X-ray crystal structure of **23** is shown in Figs. 5a and 5b and reveals that the $[\text{Mn}(\text{CO})_3]$ fragment is situated on the con-

Fig. 5. (a) Molecular structure of the $[(\eta^6\text{-dibenzosuberane})\text{Mn}(\text{CO})_3]^+$ cation in **23**, illustrating the positioning of the $\text{Mn}(\text{CO})_3$ tripod on the concave face of the ligand. (b) Bird's eye view showing the eclipsed orientation of the tripod. Thermal ellipsoids are shown at the 30% probability level.



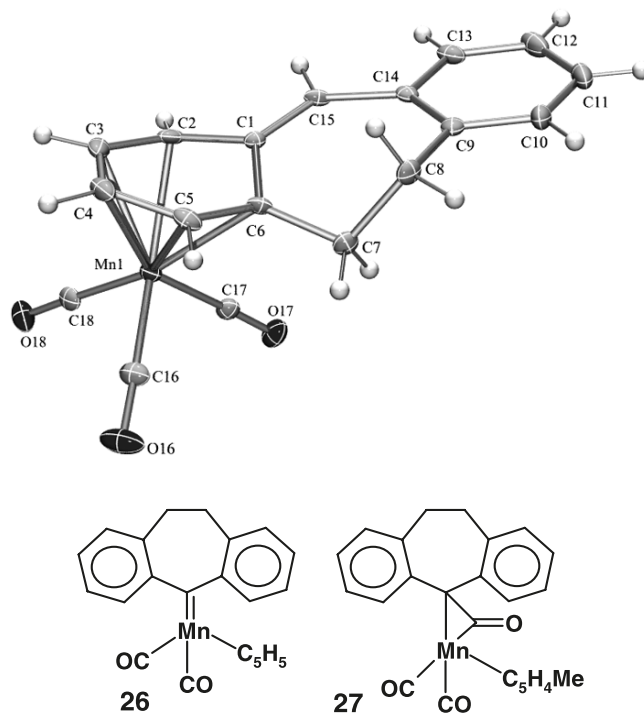
cave face of the tricyclic dibenzosuberane skeleton. The interplanar angle between the two arene rings in **23** is 129° , somewhat larger than the corresponding angle (123°) found in uncomplexed dibenzosuberane (**31**).

This result contrasts with the structures of the previously reported $(\eta^6\text{-dibenzosuberane})\text{Cr}(\text{CO})_3$ and $(\eta^6\text{-dibenzosuberone})\text{Cr}(\text{CO})_3$ in which the metal tripod lies on the exo (convex) side of the ligand, but follows the example of $(\eta^6\text{-dibenzosuberanol})\text{Cr}(\text{CO})_3$, which, like **23**, places the metal on the endo (concave) face (**32**). In the manganese case, this preference for the concave face may be a consequence of the need to pack both the organometallic cation and the tetrafluoroborate counterion as efficiently as possible.

It is common for polycyclic molecules that are π -complexed to metal fragments to fold away from the metal: examples include both α - and β - $\text{Cr}(\text{CO})_3$ complexes of *O*-methyl podocarpate (**33**), as well as ruthenium (**34**), chromium (**35**), and manganese (**26**) derivatives of estradiol and estrone. Other crystallographically characterized molecules that contain manganese and the suberane skeleton are the carbene complex, **26**, and the η^2 -ketene derivative, **27** (**36**).

Treatment of the (dibenzosuberane)tricarbonylmanganese cationic complex (**23**) with potassium *tert*-butoxide and trimethyl phosphite yielded, after chromatographic separation, a number of products in quantities too small to characterize unambiguously. Consequently, as was done in the case of $[(\eta^6\text{-tetralin})\text{Mn}(\text{CO})_3][\text{PF}_6]$, each reagent was treated separately with $[(\eta^6\text{-dibenzosuberane})\text{Mn}(\text{CO})_3][\text{BF}_4]$. Although, in the absence of light, trimethyl phosphite alone did

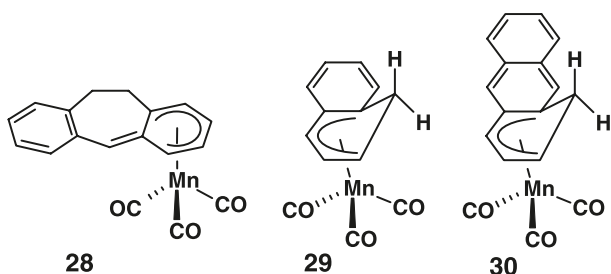
Fig. 6. Molecular structure of $(\eta^5\text{-C}_{15}\text{H}_{13})\text{Mn}(\text{CO})_3$ (**28**); thermal ellipsoids are shown at the 30% probability level.



not lead to substitution of a carbonyl ligand, the reaction of **23** with *tert*-BuOK in THF gave as the major product an orange powder exhibiting carbonyl IR absorptions at 2022 and 1950 cm^{-1} and a parent peak in the mass spectrum at m/z 332. This material was characterized by X-ray crystallography as $(\eta^5\text{-C}_{15}\text{H}_{13})\text{Mn}(\text{CO})_3$ (**28**), in which deprotonation of the benzylic proton had occurred resulting in generation of a double bond in the central seven-membered ring. The structure of compound **28** appears in Fig. 6 and shows that the metal tripod is coordinated in an η^5 -fashion to one of the outer six-membered rings, such that the manganese is located 1.718 \AA below the ring.

The manganese-dienyl carbon bond distances in **28** range from $2.126(5)$ to $2.287(5)\text{ \AA}$, typical for cyclohexadienyl manganese complexes, while the $\text{C}(1)\text{-C}(15)$ bond length of $1.358(6)\text{ \AA}$ is significantly shorter than $\text{C}(1)\text{-C}(6)$ ($1.468(6)\text{ \AA}$), and indicates double bond character. The carbon-carbon distances of the cyclohexadienyl ring average 1.407 \AA and the cyclohexadienyl unit exhibits a deviation from planarity of only 0.002 \AA , but the distortion from planarity of the cyclohexadienyl ring, i.e., the angle between planes $\text{C}(2)\text{-C}(3)\text{-C}(4)\text{-C}(5)\text{-C}(6)$ and $\text{C}(2)\text{-C}(1)\text{-C}(6)$ is 31° . This dihedral angle θ is smaller than is found in $(\eta^5\text{-C}_6\text{H}_7)\text{Mn}(\text{CO})_3$ (43°) (**37**) or *endo*- $(\eta^5\text{-C}_6\text{Me}_6\text{H})\text{Mn}(\text{CO})_2\{\text{P}(\text{OMe})_3\}$ (47.5°) (**14**) but is similar to those observed in the polycyclic systems **29** and **30**, derived from naphthalene or anthracene, in which the cyclohexadienyl ring is bent through 36° and 33° , respectively (**38**, **39**).

The product derived from the reaction of $[(\eta^6\text{-dibenzosuberane})\text{Mn}(\text{CO})_3][\text{BF}_4]$ (**23**) with potassium *tert*-butoxide is reminiscent of the behavior of the $[(\eta^6\text{-fluorene})\text{ML}_n]^+$ cation (**31**) [$\text{ML}_n = \text{Fe}(\text{C}_5\text{H}_5)$ or $\text{Mn}(\text{CO})_3$], which upon deprotonation yielded $(\eta^5\text{-fluorenyl})\text{ML}_n$, (**32**) (**40**, **41**). In principle, these neutral molecules can be represented either



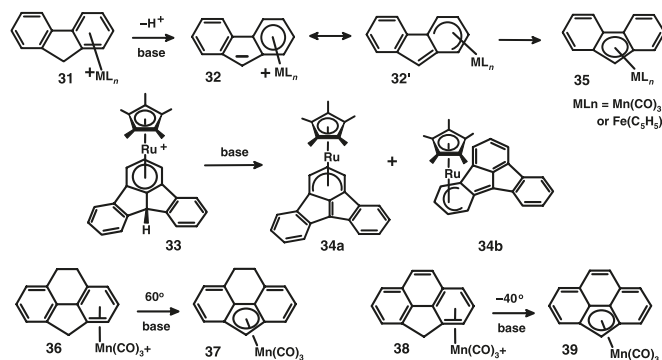
as zwitterions or as possessing a formal double bond in the central ring, as in **32'**. However, the X-ray crystal structures probably favored the latter interpretation in which the cyclohexadienyl ring is folded through 11° (Fe) or 15° (Mn), and the bond from the ring junction carbon to the benzylic carbon is 1.38 \AA (Fe) (40) or 1.37 \AA (Mn) (41). The (fluoradene)Ru(C₅Me₅) complexes **33** and **34** behave similarly (42). When (η^5 -fluorenyl)ML_{*n*} (**32**), where ML_{*n*} = Mn(CO)₃ or Fe(C₅H₅), is heated, the organometallic moiety undergoes a haptotropic shift onto the central five-membered ring to produce **35** (41). As shown in Scheme 7, analogous behavior has also been reported for the (8,9-dihydrocyclopenta[*def*]phenanthrenyl)Mn(CO)₃ complexes **36** and **37** (19). Interestingly, the η^6 -to- η^5 haptotropic shift of the organometallic fragment in the (cyclopenta[*def*]phenanthrenyl)Mn(CO)₃ complexes **38** and **39** occurs readily at -40°C , and this has been rationalized in terms of the enhanced aromatic character of the transition state (43).

Why are the reactions so different?

We must now ask ourselves why the arene–manganese tricarbonyl cations **1**, **17**, and **23** possessing five-, six-, or seven-membered rings, respectively, exhibit such different behavior when treated with *tert*-BuOK. The trindane (or indane) system apparently yields a metal hydride that subsequently suffers a series of hydrogen eliminations, presumably via agostic interactions with suitably positioned benzylic hydrogens. The tetralin complex **17** appears to undergo proton abstraction to generate a nucleophile that can attack its progenitor, whereas deprotonation of the dibenzosuberane-complexed cation **23** yielded a stable elimination product.

Evidently, there can be competition between deprotonation at a benzylic site and nucleophilic attack by the alkoxide at a carbonyl ligand. Moreover, even if a manganese-hydride were to be generated in each case, one must then consider not only the ease or difficulty of forming an agostic Mn⋯H⋯C linkage, but also the strength of the manganese-to-ligand binding subsequent to the haptotropic shift. Taking the X-ray crystallographic data for (η^6 -trindane)Mn(CO)₂Br (**3**), [(η^6 -tetralin)Mn(CO)₂{P(OMe)₃}]⁺ (**20**), and [(η^6 -dibenzosuberane)Mn(CO)₃]⁺ (**23**), we note that the Mn-to-benzylic *endo*-H distances generally lie in the range 3.42 – 3.52 \AA , considerably longer than might be anticipated for a manganese⋯hydrogen agostic interaction ($\sim 1.8 \text{ \AA}$) (44). However, manganese-hydrogen agostic interactions have been invoked by Cooper and co-workers (38) to explain the fluxional behavior of the anthracenyl complex **29** whereby an *endo* benzylic hydrogen undergoes a 1,4 migration via the metal center. In that case, the metal-hydrogen distance in the ground state was determined crystallographi-

Scheme 7. Haptotropic shifts in polycyclic systems.



cally to be 3.13 \AA , but such a process requires a flattening of the six-membered ring and an elongation of the C–H bond.

The transformation of (η^6 -trindane)Mn(CO)₂H (**5**) into (η^5 -C₁₅H₁₅)Mn(CO)₃ (**7**) involves C–H and Mn–H cleavage with concomitant formation of a manganese–carbonyl bond and two molecules of dihydrogen. The requisite bond energies are BE(C–H) 413 kJ mol^{-1} , BE(Mn–H) 288 kJ mol^{-1} [calculated value (45)], BE(H–H) 436 kJ mol^{-1} , and BE(Mn–CO) $\sim 190 \text{ kJ mol}^{-1}$ (46). Thus, cleavage of three C–H bonds and one Mn–H bond has an energy cost of approximately 1527 kJ mol^{-1} of which only $\sim 1060 \text{ kJ mol}^{-1}$ are recovered as one Mn–CO and two H–H bonds. The overall free energy change must be controlled by the stronger bonding of the manganese to the five-membered ring and, of course, by the very favorable increase in entropy brought about by the liberation of two moles of dihydrogen.

The complex [(η^6 -trindane)Mn(CO)₃]⁺ (**1**) preferentially undergoes nucleophilic attack by the *tert*-butoxide anion on a metal carbonyl ligand, whereas in the tetralin and dibenzosuberane complexes, **17** and **23**, deprotonation at a benzylic site is favored. Steric considerations would suggest that in **23** the positioning of the metal tripod on the concave face of the dibenzosuberane ligand seriously hinders the approach of a relatively bulky *tert*-butoxide; in contrast, the Mn(CO)₃ moiety in the trindane complex **1** is staggered with respect to the five-membered rings, and the alkoxide can readily gain access to a carbonyl ligand. Upon removal of a benzylic proton from [(η^6 -dibenzosuberane)Mn(CO)₃]⁺, the resulting neutral species **28** is sufficiently flexible to allow the seven-membered ring to fold away from the metal and so adopt a conventional η^5 -cyclohexadienyl conformation; this molecular deformation may be more difficult for the deprotonated tetralene complex **22**, which therefore retains its nucleophilic character and attacks the starting material to yield the “dimeric tetralenyl” η^5 -cyclohexadienyl product **21**.

To conclude, the reactions of potassium *tert*-butoxide with the arene manganese tricarbonyl cations derived from trindane, indane, tetralin, or dibenzosuberane yield very different products and pose interesting mechanistic questions.

Experimental section

General procedures

All reactions were carried out under an atmosphere of dry nitrogen employing conventional benchtop and glovebag techniques. Silica gel (particle size 20 – $45 \mu\text{m}$) was employed for flash column chromatography. Radial chromatog-

raphy was performed using a Chromatotron (7942T, Harrison Research, Inc.) with silica-coated plates (TLC grade 7749 with gypsum binder and fluorescent indicator; thickness: 1, 2, or 4 mm). ^1H , ^{13}C , and ^{31}P NMR data were acquired on Bruker Avance 500, 300, or 200 MHz spectrometers, and chemical shifts are given relative to residual ^1H or ^{13}C solvent signal, or externally referenced relative to 85% H_3PO_4 in D_2O . IR spectra were recorded on a Bio-Rad FTS-40 single beam spectrometer using KBr pellets or NaCl windows. In situ IR spectra were recorded on an ASI Applied Systems ReactIR 1000 with a SiComp probe. Mass spectrometric data were obtained on a Finnigan EI/CI mass spectrometer system, using direct electron impact and chemical ionization methods. The positive ion electrospray mass spectra were obtained on a Micromass Quattro LC triple quadrupole mass spectrometer. Melting and decomposition points were measured on a Fischer-Johns melting point apparatus and are not corrected. Microanalytical data are from Guelph Chemical Laboratories (Guelph, Ontario) or from the Microanalytical Laboratory at University College Dublin.

$[(\eta^6\text{-Trindane})\text{Mn}(\text{CO})_3][\text{BF}_4]$ (**1**) and $[(\eta^6\text{-trindane})\text{Fe}(\text{C}_5\text{H}_5)][\text{PF}_6]$ (**2**) were prepared as previously described (2). Following the literature procedure (47), dibenzosuberane was obtained in 77% yield by reduction of dibenzosuberone with iodine and hypophosphorous acid in acetic acid.

Reaction of $[(\eta^6\text{-trindane})\text{Mn}(\text{CO})_3][\text{BF}_4]$ with *tert*-BuOK and allyl bromide

A three-neck round-bottomed flask equipped with a side-arm, condenser, septum, and stir bar was charged with $[(\eta^6\text{-trindane})\text{Mn}(\text{CO})_3][\text{BF}_4]$ (**1**) (0.500 g, 1.18 mmol) and *tert*-BuOK (1.33 g, 11.87 mmol) and held under vacuum for 3 h at 40 °C. A solution of allyl bromide (1.02 mL, 11.8 mmol) in THF (25 mL) was added via cannula, under N_2 , and produced a green solution that was maintained at 40 °C, which eventually turned brownish-orange. After 20.5 h, the solvent was removed under reduced pressure and the pinkish-red residue was dissolved in CH_2Cl_2 , filtered, and extracted with H_2O (3 × 10 mL). The organic layers were combined, dried with Na_2SO_4 , and filtered, and the solvent was removed by rotary evaporation. After drying under vacuum, **3** was obtained as a dark red powder (0.077 g, 0.198 mmol; 17%), mp 128–130 °C (dec). IR (NaCl windows, CDCl_3 , cm^{-1}) ν_{CO} : 1971(s), 1927 (s). ^1H NMR (200 MHz, CD_2Cl_2) δ : 2.76 (br, 12H, benzylic CH_2), 2.04 (br, 6H, wingtip CH_2). ^{13}C NMR (50 MHz, CD_2Cl_2) δ : 110.3 (aromatic C), 30.1 (benzylic CH_2), 24.1 (wingtip CH_2). Mass spectrum (MS) (DEI, m/z (%)): 198 (100, $[\text{C}_{15}\text{H}_{18}]^+$), 115 (5, $[\text{C}_9\text{H}_7]^+$). (As with $(\text{C}_6\text{Me}_6)\text{Mn}(\text{CO})_2\text{Br}$, no parent ion was detectable; only peaks attributable to the ligand were observed.) Anal. calcd. for $\text{C}_{17}\text{H}_{18}\text{MnBrO}_2$ (%): C 52.47, H 4.66; found: C 52.04, H 4.92. A crystal suitable for an X-ray diffraction study was obtained by slow evaporation of dichloromethane at room temperature under an atmosphere of nitrogen.

Alternative route to $(\eta^6\text{-trindane})\text{Mn}(\text{CO})_2\text{Br}$ (**3**)

The second synthesis of **3** is based on the previously reported preparation of $(\eta^6\text{-C}_6\text{Me}_6)\text{Mn}(\text{CO})_2\text{Br}$ (**12**). $[(\eta^6\text{-Trindane})\text{Mn}(\text{CO})_3][\text{BF}_4]$ (0.501 g, 1.18 mmol), Me_3NO (0.107 g, 1.29 mmol), and $(n\text{-Bu})_4\text{NBr}$ (0.566 g, 1.433 mmol) were combined in a two-neck round-bottomed

flask. The system was evacuated, flushed with N_2 (three times), and CH_2Cl_2 (25 mL) was added. The resulting red solution was left to stir under N_2 for 2 h, after which time the solvent was removed under reduced pressure. The crude product was chromatographed on a silica gel column (eluent hexane/acetone 50:50) affording **3** (0.425 g, 1.092 mmol, 93%). NOTE: trimethylamine *N*-oxide hydrate ($\text{Me}_3\text{NO}\cdot 2\text{H}_2\text{O}$) was dehydrated by azeotroping the water from a toluene solution.

Reaction of $[(\eta^6\text{-trindane})\text{Mn}(\text{CO})_3][\text{BF}_4]$ with *tert*-BuOK and methyl iodide

Analogously to the preparation of **3**, $[(\eta^6\text{-trindane})\text{Mn}(\text{CO})_3][\text{BF}_4]$ (0.513 g, 1.21 mmol), *tert*-BuOK (2.65 g, 23.6 mmol), and methyl iodide (1.47 mL, 23.6 mmol) in THF (25 mL) produced a purple solution that eventually turned yellow-cream. Work-up was as above, and separation by rotary chromatography (Chromatotron, eluent hexane/ CH_2Cl_2 20:80) yielded $(\eta^6\text{-trindane})\text{Mn}(\text{CO})_2\text{I}$ (**4**) (0.078 g, 0.18 mmol; 15%). IR (NaCl windows, CDCl_3 , cm^{-1}) ν_{CO} : 1973 (s), 1926 (s). ^1H NMR (500 MHz, CDCl_3) δ : 2.80 (m, 12H, benzylic CH_2), 2.09 (br, 6H, wingtip CH_2). ^{13}C NMR (125 MHz, CDCl_3) δ : 108.8 (aromatic C), 30.1 (benzylic CH_2), 23.7 (wingtip CH_2). MS (DEI, m/z (%)): 380 (40, $[\text{M} - 2\text{CO}]^+$), 253 (10, $[\text{M} - 2\text{CO} - \text{I}]^+$), 198 (100, $[\text{C}_{15}\text{H}_{18}]^+$). Anal. calcd. for $\text{C}_{17}\text{H}_{18}\text{MnIO}_2$ (%): C 46.81, H 4.16; found: C 47.02, H 4.32. A crystal suitable for an X-ray diffraction study was obtained by slow evaporation of dichloromethane at room temperature under an atmosphere of nitrogen.

Reaction of $[(\eta^6\text{-trindane})\text{Mn}(\text{CO})_3][\text{BF}_4]$ with *tert*-BuOK and trimethyl phosphite

Likewise, $[(\eta^6\text{-trindane})\text{Mn}(\text{CO})_3][\text{BF}_4]$ (0.500 g, 1.18 mmol), *tert*-BuOK (2.65 g, 23.6 mmol), and $\text{P}(\text{OMe})_3$ (2.78 mL, 23.6 mmol) in THF (30 mL) produced a red solution that eventually turned orange-brown. Workup was as above, and chromatography on a silica gel column (eluent hexane/ CH_2Cl_2 70:30) yielded two fractions, $(\eta^5\text{-C}_{15}\text{H}_{15})\text{Mn}(\text{CO})_3$ (**7**) (0.080 g, 0.240 mmol; 20%), mp 87–90 °C and $(\eta^5\text{-C}_{15}\text{H}_{15})\text{Mn}(\text{CO})_2\text{P}(\text{OMe})_3$ (**8**) (0.055 g, 0.130 mmol; 11%), mp 124–126 °C.

Data for **7**: ^1H NMR (200 MHz, CDCl_3) δ : 5.03 (d, 2H, CH), 4.94 (t, 1H, CH), 2.93 (m, 4H, benzylic CH_2), 2.79 (m, 4H, benzylic CH_2), 2.13 (m, 4H, wingtip CH_2). ^{13}C NMR (50 MHz, CDCl_3) δ : 225.4 (Mn-CO), 139.4 (C6/C9 or C7/C8, C=C), 135.2 (C6/C9 or C7/C8, C=C), 101.1 (C4/C5), 87.4 (C2, CH), 69.7 (C1/C3, CH), 32.1 (benzylic CH_2), 25.5 (wingtip CH_2), 32.1 (benzylic CH_2). Anal. calcd. for $\text{C}_{18}\text{H}_{15}\text{MnO}_3$ (%): C 64.68, H 4.52; found: C 65.01, H 4.67. After numerous attempts, yellow crystals were grown from chloroform at 0 °C under an atmosphere of nitrogen, but were not of ideal quality. Nevertheless, an X-ray diffraction study was undertaken and the molecular structure was determined.

Data for **8**: IR (NaCl windows, CDCl_3 , cm^{-1}) ν_{CO} : 1944 (s), 1876 (s). ^1H NMR (500 MHz, CDCl_3) δ : 4.84 (m, 3H, CH), 3.38 (d, $^3J_{\text{H,P}} = 11.7$ Hz, 9H, OCH_3), 3.04 (m, 2H, benzylic CH_2), 2.92 (m, 2H, benzylic CH_2), 2.84 (m, 2H, benzylic CH_2), 2.75 (m, 2H, benzylic CH_2), 2.16 (m, 4H, wingtip CH_2). ^{13}C NMR (125 MHz, CDCl_3) δ : 137.9 (C6/C9 or C7/C8, C=C), 135.8 (C6/C9 or C7/C8, C=C), 100.9

(C4/C5), 87.0 (C2, CH), 68.7 (C1/C3, CH), 51.1 (OCH₃), 32.2 (benzylic CH₂), 31.8 (benzylic CH₂), 24.6 (wingtip CH₂). ³¹P NMR (81.04 MHz, CDCl₃) δ: 211.6 (s). MS (DEI, *m/z* (%)): 430 (11, [M]⁺), 374 (100, [M - 2CO]⁺), 281 (21, [M - 2CO - 3(OMe)]⁺), 251 (51, [M - 2CO - P(OMe)₃]⁺), 195 (44, [(C₁₅H₁₅)]⁺). Anal. calcd. for C₂₀H₂₄MnO₃P (%): C 55.82, H 5.62; found: C 55.45, H 5.96. A yellow crystal suitable for an X-ray diffraction study was grown from chloroform at 0 °C under an atmosphere of nitrogen.

Reaction of [(η⁶-trindane)Mn(CO)₃][BF₄] with *tert*-BuOK and triphenylphosphine

Analogously to the preparation of **8**, [(η⁶-trindane)Mn(CO)₃][BF₄] (0.500 g, 1.182 mmol), *tert*-BuOK (2.65 g, 23.6 mmol), THF (30 mL), and PPh₃ (619 g, 23.6 mmol) yielded three fractions after separation on a Chromatron (eluent hexane/CH₂Cl₂ 90:10): PPh₃, (η⁵-C₁₅H₁₅)Mn(CO)₃ (**7**), and (η⁵-C₁₅H₁₅)Mn(CO)₂[PPh₃] (**9**) (0.060g, 0.1056 mmol; 9%), mp 179–180 °C (dec). IR (NaCl windows, CDCl₃, cm⁻¹) ν_{CO}: 1929 (s), 1862 (s). ¹H NMR (500 MHz, CDCl₃) δ: 7.31 (m, 15H, aromatic CH), 4.60 (d, 2H, CH), 4.47 (m, 1H, CH), 2.51 (m, 8H, benzylic CH₂), 2.08 (m, 4H, wingtip CH₂). ¹³C NMR (125 MHz, CDCl₃) δ: 138.1, 137.8, 136.1, 133.1 (*J*_{C-P} = 10.4 Hz), 129.5, 128.1 (*J*_{C-P} = 9.3 Hz), 100.7 (C4/C5), 89.0 (C2, CH), 70.7 (C1/C3, CH), 32.3 (benzylic CH₂), 32.0 (benzylic CH₂), 24.6 (wingtip CH₂). ³¹P NMR (81.04 MHz, CDCl₃) δ: 94.3. MS (DEI, *m/z* (%)): 569 (100, [M + H]⁺), 512 (58, [M - 2CO]⁺), 195 (62, [C₁₅H₁₅]⁺); (CI, NH₃, *m/z* (%)): 569 (100, [M + H]⁺), 512 (58, [M - 2CO]⁺), 195 (63, [C₁₅H₁₅]⁺). Anal. calcd. for C₃₅H₃₀MnO₂P (%): C 73.94, H 5.28; found: C 74.18, H 5.49.

Preparation of [(η⁶-indane)Mn(CO)₃][BF₄] (**10**)

A mixture of Mn(CO)₅Br (1.08 g, 4.029 mmol) and AgBF₄ (0.78 g, 4.029 mmol) in dry CH₂Cl₂ (40 mL) was heated at reflux for 3 h under nitrogen and then cooled to room temperature. To the reaction mixture, a solution of indane (0.493 mL, 4.029 mmol) in dry CH₂Cl₂ (10 mL) was added, and the reaction mixture was heated at reflux for 18 h. After cooling and filtration, the filtrate was passed through Celite and concentrated to approximately one-third its volume under reduced pressure, and excess hexane (80 mL) was added. The resulting yellow solid was filtered and dried in vacuo to furnish **10** (0.658 g, 1.918 mmol, 50%). IR (NaCl windows, CDCl₃, cm⁻¹) ν_{CO}: 2065 (s), 2008 (s). ¹H NMR (200 MHz, CD₂Cl₂) δ: 6.53 (m, 4H, aromatic), 3.03 (m, 4H, benzylic CH₂), 2.44 (m, 1H, wingtip CH₂), 2.10 (m, 1H, wingtip CH₂). ¹³C NMR (50 MHz, CD₂Cl₂) δ: 227.2 (Mn-CO), 99.3 (aromatic C), 98.2 (aromatic C), 32.2 (benzylic CH₂), 23.7 (wingtip CH₂). MS (positive ESI, *m/z* (%)): 258 (M + 1, 24% of [M]⁺), 257 (100, [M]⁺), 229 (5.3, [M - CO]⁺), 201 (2.7, [M - 2CO]⁺), 173 (1.9, [M - 3CO]⁺). Anal. calcd. for C₁₂H₁₀O₃MnBF₄ (%): C 41.90, H 2.93; found: C 41.69, H 2.76.

Reaction of [(η⁶-indane)Mn(CO)₃][BF₄] with *tert*-BuOK and triphenylphosphine

Following the procedure for **3**, [(η⁶-indane)Mn(CO)₃][BF₄] (0.106 g, 0.3089 mmol), *t*-BuOK (0.693 g, 6.178 mmol), and PPh₃ (1.620 g, 6.178 mmol) in THF

(35 mL) produced a reddish-orange solution. Work-up yielded (η⁵-indanyl)Mn(CO)₂PPh₃ (0.017 g, 0.0348 mmol, 11%). IR (NaCl windows, CDCl₃, cm⁻¹) ν_{CO}: 1934 (s), 1866 (s), lit. (18); (nujol) ν_{CO}: 1931(s), 1863 (s). ¹H NMR (300 MHz, CD₂Cl₂) δ: 7.09 (m, 19H, aromatic C and CH=CH), 4.65 (m, 3H, Cp). ¹³C NMR (75 MHz, CDCl₃) δ: 232.8 (Mn-CO), 133.7, 133.5, 130.1, 128.6, 128.5, 126.1, 125.9, 90.1 (Cp), 72.9 (Cp). ³¹P NMR (81.05 MHz, CD₂Cl₂) δ: 92.4 (s). MS (DEI, *m/z* (%)): 488 (6, [M]⁺), 432 (92, [M - 2CO]⁺), 377 (1, [M - 2CO - Mn]⁺), 115 (100, [C₉H₇]⁺).

Reaction of [(η⁶-indane)Mn(CO)₃][BF₄] with *tert*-BuOK and trimethyl phosphite

As for the reaction with triphenylphosphine, [(η⁶-indane)Mn(CO)₃][BF₄] (0.500 g, 1.457 mmol), *t*-BuOK (3.27 g, 29.0 mmol), and P(OMe)₃ (619 g, 23.6 mmol) in THF (30 mL) yielded (η⁵-indanyl)Mn(CO)₂[P(OMe)₃] (0.001 g, 2.857 mmol, 2%). IR (NaCl windows, CDCl₃, cm⁻¹) ν_{CO}: 1950 (s), 1881 (s). ¹H NMR (200 MHz, CDCl₃) δ: 7.40 (m, 2H, CH=CH), 7.02 (m, 2H, CH=CH), 4.97 (m, 2H, CH), 4.83 (m, 1H, CH), 3.42 (d, 9H, ³*J*_{C-P} = 11.7 Hz, OCH₃). ³¹P NMR (81.05 MHz, CD₂Cl₂) δ: 211.4 (s). MS (DEI, *m/z* (%)): 350 (12, [M]⁺), 322 (5, [M - CO]⁺), 294 (100, [M - 2CO]⁺), 170 (29, [C₉H₇Mn]⁺), 115 (41, [C₉H₇]⁺).

Preparation of [(η⁶-trindane)Mn(CO){P(OMe)₃}]₂[BF₄] (**15**)

[(η⁶-Trindane)Mn(CO)₃][BF₄] (0.463 g, 1.095 mmol) and Me₃NO (0.173 g, 2.307 mmol) were stirred in CH₂Cl₂ (55 mL) under N₂. To the yellow solution was added P(OMe)₃ (0.20 mL, 1.696 mmol) whereupon the solution turned red instantaneously. The solution was allowed to stir under N₂ for 6 h at room temperature, the solvent was removed under pressure, and the crude material was purified by chromatographic separation on a silica gel column (eluent CH₂Cl₂/acetone 90:10) giving rise to two fractions. The first fraction was identified as trindane and the second was **15** (0.071 g, 0.115 mmol, 11%). IR (NaCl windows, CDCl₃, cm⁻¹) ν_{CO}: 1911 (s). ¹H NMR (300 MHz, CD₂Cl₂) δ: 3.71 (t, 18H, ³*J*_{P-H} = 5.0 Hz, P(OMe)₃), 2.74 (m, 12H, benzylic CH₂), 2.08 (m, 6H, wingtip CH₂). ¹³C NMR (75 MHz, CD₂Cl₂) δ: 111.7 (aromatic C), 54.5 (OCH₃), 30.4 (benzylic CH₂), 23.2 (wingtip CH₂). ³¹P NMR (121.51 MHz, CD₂Cl₂) δ: 185.5 (s). MS (positive ESI, *m/z* (%)): 529 (100, [M]⁺), 405 (3, [M - P(OMe)₃]⁺), 377 (8, [M - P(OMe)₃ - CO]⁺). Anal. calcd. for C₂₂H₃₆MnO₇P₂ (%): C 42.88, H 5.89; found: C 42.69, H 5.86. A sample suitable for single-crystal X-ray diffraction was obtained by crystallization from dichloromethane by slow evaporation under nitrogen at room temperature.

Preparation of [(η⁶-trindane)Re(CO)₃][PF₆] (**16**)

In a 100 mL round-bottomed flask, BrRe(CO)₅ (0.944 g, 2.324 mmol), trindane (0.765 g, 3.864 mmol), AlCl₃ (1.630 g, 12.22 mmol), and petroleum ether (55 mL) were heated at reflux under nitrogen for 16.5 h. The solution was cooled in an ice-bath, followed by addition of an ice-water slush (25 mL). The petroleum ether layer was decanted, and the remaining water layer was washed with cold diethyl ether followed by the addition of excess NH₄PF₆ in water (5 mL). The resultant white precipitate (0.028 g, 0.0456 mmol, 2%) was filtered and washed with cold water

and methanol. IR (KBr pellet, cm^{-1}) ν_{CO} : 2052 (s), 1956 (s). IR (NaCl windows, CDCl_3 , cm^{-1}) ν_{CO} : 2058 (s), 1966 (s). ^1H NMR (500 MHz, CD_2Cl_2) δ : 3.38 (m, 6H, benzylic CH_2), 2.95 (m, 6H, benzylic CH_2), 2.44 (m, 3H, wingtip CH_2), 1.91 (m, 3H, wingtip CH_2). ^{13}C NMR (125.773 MHz, CD_2Cl_2) δ : 185.7 (Mn-CO), 118.7 (aromatic C), 30.4 (benzylic CH_2), 24.7 (wingtip CH_2). MS (positive ESI, m/z (%)): 469 (100, $[\text{M}]^+$).

Attempted synthesis of $[(\eta^6\text{-}(\text{CH}_3)_{12}\text{C}_{15}\text{H}_6)\text{FeCp}][\text{PF}_6]$

$[(\eta^6\text{-C}_{15}\text{H}_{18})\text{FeCp}][\text{PF}_6]$ (**2**) (0.124 g, 0.267 mmol) and potassium *tert*-butoxide (7.20 g, 64 mmol) were stirred together under vacuum for 3 h, and a solution of methyl iodide (3.98 mL, 64 mmol) in freshly distilled THF (60 mL) was introduced by syringe. The solution became deep red in colour and continued to change colour (dark purple to mauve to pink) until the solution remained yellowish-cream in colour. After 48 h under nitrogen at 40 °C in the dark, the product was worked up as before, and chromatographed on an alumina neutral column (eluent hexane/acetone 90:10) to afford three orange products. The ^1H and ^{13}C NMR spectra of each fraction still indicated a mixture of compounds. Similarly positive ESI mass spectrometric data exhibited signals at m/z 459, 473, and 487 corresponding to the incorporation of 10, 11, and 12 methyls, respectively. Two samples suitable for structural determination by single-crystal X-ray diffraction were obtained by recrystallization from hexanes/acetone mixture; however, the structure has not been satisfactorily refined as a result of a disorder in the trindane fragment.

Attempted synthesis of $[(\eta^6\text{-}(\text{CH}_2\text{CHCH}_2)_{12}\text{C}_{15}\text{H}_6)\text{FeCp}][\text{PF}_6]$

Similarly, $[(\eta^6\text{-C}_{15}\text{H}_{18})\text{FeCp}][\text{PF}_6]$, **2**, (0.233 g, 0.502 mmol), potassium *tert*-butoxide (13.5 g, 120 mmol), and allyl bromide (10.43 mL, 120 mmol) in THF (60 mL) became deep red in colour and continued to change colour (pink to violet to mauve) until the solution remained yellowish-cream in colour. After work-up, the crude product was chromatographed on an alumina neutral column (eluent hexane) affording two yellow products. The ^1H and ^{13}C NMR spectra of each fraction still indicated a mixture of compounds. Similarly positive ESI mass spectrometric data exhibited signals consistent with the incorporation of 12 allyl groups at m/z 799, followed by consecutive losses of multiples of 40 to a m/z of 319 (which corresponds to $[(\eta^6\text{-C}_{15}\text{H}_{18})\text{FeCp}]^+$).

Preparation of $[(\eta^6\text{-tetralin})\text{Mn}(\text{CO})_3][\text{PF}_6]$ (**17**)

As described in the literature (25), $\text{Mn}(\text{CO})_5\text{Br}$ (1.97 g, 7.16 mmol), AlCl_3 (1.91 g, 14.3 mmol), tetralin (1.88 mL, 0.0138 mmol), and cyclohexane (50 mL) were heated at reflux for 5 h under N_2 . The solution was cooled, followed by the addition of ice-cold H_2O (40 mL). To the aqueous layer, NH_4PF_6 (2.21 g, 0.0138 mmol) was added, yielding a yellow precipitate that was filtered and dried under vacuum. The product (2.383 g, 5.73 mmol, 80%) was recrystallized from a mixture of acetone and diethyl ether. Complete spectroscopic assignment of this compound had not been published prior to this study. IR (NaCl windows, CDCl_3 , cm^{-1}) ν_{CO} : 2068 (s), 2025 (s), 2003 (s), lit. (25) (NaCl) ν_{CO} : 2056 (s), 2016 (s). ^1H NMR (200 MHz, acetone- d_6) δ : 6.84 (s, 4H, CH), 3.13 (m, 4H, CH_2), 2.30 (m, 4H, CH_2). ^{13}C NMR (50 MHz, acetone- d_6) δ : 216.9, 119.5, 101.9, 99.8, 28.2,

21.6. MS (positive ESI, m/z (%)): 271 (100, $[\text{M}]^+$), 243 (8, $[\text{M} - \text{CO}]^+$), 214 (23, $[\text{M} - 2\text{CO}]^+$), 187 (7, $[\text{M} - 3\text{CO}]^+$).

Reaction of $[(\eta^6\text{-tetralin})\text{Mn}(\text{CO})_3][\text{PF}_6]$ with trimethyl phosphite

A 100 mL Schlenk flask equipped with a side arm and stir bar was charged with $[(\eta^6\text{-tetralin})\text{Mn}(\text{CO})_3][\text{PF}_6]$ (**17**) (0.902 g, 2.168 mmol) and evacuated and purged with N_2 three times. A solution of THF (30 mL) containing $\text{P}(\text{OMe})_3$ (5.11 mL, 43.4 mmol) was added dropwise under N_2 , the solution was yellow in colour. The solution was stirred for 20 h under N_2 and the solvent was then removed under reduced pressure. The residue was dissolved in CH_2Cl_2 and hexanes, a precipitate formed, and it was filtered. The remaining solution was chromatographed on a silica gel column (eluent 100% hexane) affording **20**, a yellow compound (0.658 g, 1.285 mmol, 59%), mp 86–88 °C. IR (NaCl windows, CDCl_3 , cm^{-1}) ν_{CO} : 2008 (s), 1961 (s). ^1H NMR (200 MHz, CDCl_3) δ : 5.94 (m, 4H, aromatic CH), 3.70 (t, 9H, $^3J_{\text{H-P}} = 11.6$ Hz, OCH_3), 2.73 (m, 4H, CH_2), 1.79 (m, 4H, CH_2). ^{13}C NMR (50 MHz, CDCl_3) δ : 220.3 (d, $^2J_{\text{C-P}} = 43.2$ Hz, Mn-CO), 113.9 (C1/C6), 97.8 (C2/C5 or C3/C4), 96.7 (C2/C5 or C3/C4), 54.1 (d, $^2J_{\text{C-P}} = 7.3$ Hz, OCH_3), 27.5 (C7/C10), 21.1 (C7/C10). ^{31}P NMR (81.04 MHz, CDCl_3) δ : 182.1 (s, $\text{P}(\text{OMe})_3$), -167.4 (septet, PF_6). MS (positive ESI, m/z (%)): 367 (100, $[\text{M}]^+$), 311 (19, $[\text{M} - 2\text{CO}]^+$). Anal. calcd. for $\text{C}_{15}\text{H}_{21}\text{MnO}_5\text{P}_2\text{F}_6$ (%): C 35.17, H 4.13; found: C 35.51, H 3.96. A sample suitable for single-crystal X-ray diffraction was obtained by crystallization from chloroform by slow evaporation under an atmosphere of nitrogen at room temperature.

Reaction of $[(\eta^6\text{-tetralin})\text{Mn}(\text{CO})_3][\text{PF}_6]$ with *tert*-BuOK

A round-bottomed flask equipped with a side arm and stir bar was charged with $[(\eta^6\text{-tetralin})\text{Mn}(\text{CO})_3][\text{PF}_6]$ (**17**) (0.952 g, 2.288 mmol) and *t*-BuOK (5.14 g, 45.8 mmol) and evacuated and purged with N_2 three times. This was followed by the addition of THF (30 mL) under N_2 , which produced a dark orange-brown solution, which was stirred for 6 h under N_2 . The solvent was removed under reduced pressure and the residue was dissolved in methylene chloride. Hexanes were added to the solution and, after filtration, the solvent was removed by rotary evaporation yielding a yellow-orange oil that was separated on a Chromatotron (eluent hexane with gradual addition of CH_2Cl_2) furnishing **21** (0.114 g, 0.284 mmol, 12%). IR (NaCl windows, neat, cm^{-1}) ν_{CO} : 2007 (s), 1927 (s). MS (CI, NH_3 , m/z (%)): 403 (100, $[\text{M} + 1]^+$), 271 (57, $[\text{M} - \text{C}_{10}\text{H}_{11}]^+$), 187 (3, $[\text{M} - \text{C}_{10}\text{H}_{11} - 3\text{CO}]^+$), 131 (8, $[\text{C}_{10}\text{H}_{11}]^+$).

Preparation of $[(\eta^6\text{-dibenzosuberane})\text{Mn}(\text{CO})_3][\text{BF}_4]$ (**23**)

A mixture of $\text{Mn}(\text{CO})_5\text{Br}$ (1.90 g, 6.92 mmol) and AgBF_4 (1.48 g, 7.61 mmol) in dry CH_2Cl_2 (50 mL) was heated at reflux for 3 h under nitrogen and then cooled to room temperature. To the reaction was added a solution of dibenzosuberane (1.78 g, 9.20 mmol) in dry CH_2Cl_2 (15 mL), and the mixture was heated at reflux overnight. After cooling and filtration, the filtrate was passed through Celite and concentrated to approximately one-third its volume under reduced pressure, and excess hexane (100 mL)

Table 1. Crystallographic collection and refinement parameters for **3**, **4**, **7**, and **8**.

Compound	3	4	7	8
Empirical formula	C ₁₇ H ₁₈ O ₂ BrMn	C ₁₇ H ₁₈ O ₂ IMn	C ₁₈ H ₁₅ O ₃ Mn	C ₂₀ H ₂₄ O ₃ PMn
Formula weight	389.16	436.15	334.24	430.30
Temperature (K)	299(2)	299(2)	173(2)	299(2)
Wavelength (Å)	0.71073	0.71073	0.71073	0.71073
Crystal system	Monoclinic	Orthorhombic	Monoclinic	Monoclinic
Space group	<i>P</i> 2 ₁ / <i>c</i>	<i>Pbca</i>	<i>C</i> 2/ <i>c</i>	<i>P</i> 2 ₁ / <i>c</i>
<i>a</i> (Å)	9.8049(13)	14.408(3)	16.567(18)	9.7325(17)
<i>b</i> (Å)	8.8852(13)	15.080(2)	9.919(14)	22.355(4)
<i>c</i> (Å)	18.682(3)	15.264(3)	18.524(26)	9.6052(17)
α (°)	90	90	90	90
β (°)	94.825(3)	90	98.09(5)	106.484(5)
γ (°)	90	90	90	90
Volume (Å ³)	1621.8(4)	3316.4(10)	3013.7(68)	2003.9(6)
<i>Z</i>	4	8	8	4
<i>D</i> _{calcd.} (Mg/m ³)	1.594	1.747	1.473	1.426
Absorption coefficient (mm ⁻¹)	3.278	2.659	0.885	0.766
<i>F</i> (000)	784	1712	1376	896
Crystal size (mm)	0.06 × 0.08 × 0.24	0.14 × 0.28 × 0.33	0.04 × 0.22 × 0.42	0.08 × 0.33 × 0.35
Theta range for data collection (°)	2.08–23.25	2.37–24.99	2.40–24.99	1.82–27.50
Index ranges	–10 ≥ <i>h</i> ≥ 10 –9 ≥ <i>k</i> ≥ 9 –20 ≥ <i>l</i> ≥ 20	–16 ≥ <i>h</i> ≥ 17 –17 ≥ <i>k</i> ≥ 17 –18 ≥ <i>l</i> ≥ 18	–21 ≥ <i>h</i> ≥ 20 –7 ≥ <i>k</i> ≥ 11 –21 ≥ <i>l</i> ≥ 16	–12 ≥ <i>h</i> ≥ 12 –28 ≥ <i>k</i> ≥ 26 –12 ≥ <i>l</i> ≥ 11
Reflections collected	10 041	23 135	2 507	17 829
Independent reflections	2318 [<i>R</i> (int) = 0.0907]	2919 [<i>R</i> (int) = 0.0323]	1717 [<i>R</i> (int) = 0.2486]	4584 [<i>R</i> (int) = 0.0300]
Absorption correction	SADABS	SADABS	SADABS	SADABS
Refinement method	Full-matrix least-squares on <i>F</i> ²	Full-matrix least-squares on <i>F</i> ²	Full-matrix least-squares on <i>F</i> ²	Full-matrix least-squares on <i>F</i> ²
Data/restraints/parameters	2318/0/191	2919/0/192	1679/0/199	4584/0/245
Goodness-of-fit on <i>F</i> ²	1.075	1.053	1.080	1.030
Final <i>R</i> indices [<i>I</i> > 2σ(<i>I</i>)]	<i>R</i> 1 = 0.0560, <i>wR</i> 2 = 0.1326	<i>R</i> 1 = 0.0412, <i>wR</i> 2 = 0.1159	<i>R</i> 1 = 0.1455, <i>wR</i> 2 = 0.3683	<i>R</i> 1 = 0.0350, <i>wR</i> 2 = 0.0876
<i>R</i> indices (all data)	<i>R</i> 1 = 0.1070, <i>wR</i> 2 = 0.1582	<i>R</i> 1 = 0.0490, <i>wR</i> 2 = 0.1237	<i>R</i> 1 = 0.1943, <i>wR</i> 2 = 0.4620	<i>R</i> 1 = 0.0528, <i>wR</i> 2 = 0.0947
Extinction coefficient	0.0000(5)		0.0000(9)	
Absolute structure parameter				
Largest diff. peak and hole (e ⁻ Å ⁻³)	0.464 and –0.436	0.756 and –0.1292	1.304 and –1.241	0.252 and –0.214

was added. The resulting yellow solid was filtered and dried under vacuum furnishing **23** (0.301 g, 0.718 mmol, 10%), mp 218–220 °C. IR (NaCl windows, CDCl₃, cm⁻¹) ν_{CO}: 2065 (s), 2014 (s). ¹H NMR (500 MHz, acetone-*d*₆) δ: 7.38 (d, 1H, *J* = 7.3 Hz, H7/H10), 7.31 (m, 2H, H8, H9), 7.25 (t, 1H, *J* = 7.1, H7/H10), 7.13 (d, 1H, *J* = 6.6 Hz, H1/H4), 6.91 (t, 1H, *J* = 6.3 Hz, H2/H3), 6.58 (t, 2H, *J* = 6.3 Hz, H1/H3 or H2/H4), 4.48 (d, 1H, *J* = 15.5 Hz, H11a/H11b), 4.31 (d, 1H, *J* = 15.5 Hz, H11a/H11b), 3.44 (m, 3H, H6a/H6b, H5a/H5b), 3.27 (m, 1H, H6a/H6b, H5a/H5b). ¹³C NMR (125 MHz, acetone-*d*₆) δ: 216.4 (Mn-CO), 139.6 (C12/C15), 138.6 (C12/C15), 130.2 (C8/C9), 129.8 (C7/C10), 129.4 (C8/C9), 128.0 (C7/C10), 123.7 (C14/C15), 118.6 (C14/C15), 105.5 (C1/C4), 103.1 (C2/C3), 100.6 (C2/C3), 97.3 (C2/C3 or C2/C4), 38.4 (C11), 32.1 (C5/C6). MS (positive ESI, *m/z* (%)): 333 (100, [M⁺]), 277 (6.15, [M – 2CO]⁺), 249 (17.75, [M – 3CO]⁺). Anal. calcd. for C₁₈H₁₄MnO₃BF₄ (%): C 51.47, H 3.36; found: C 51.48, H 3.51. A sample suitable for structural determination by

single-crystal X-ray diffraction was obtained by crystallization from acetone at room temperature.

Reaction of [(η⁶-dibenzosuberane)Mn(CO)₃][BF₄] with *tert*-BuOK

A round-bottomed flask equipped with a side arm and stir bar was charged with [(η⁶-dibenzosuberane)Mn(CO)₃][BF₄] (**23**) (0.377 g, 0.90 mmol) and *t*-BuOK (2.02 g, 18.0 mmol) and evacuated and purged with N₂ three times. This was followed by the addition of THF (25 mL) under N₂, which produced a dark red-brown-orange solution, which was stirred for 4 h under N₂. The solvent was removed under reduced pressure and the residue was dissolved in ether. Water (40 mL) was added to the ether solution and extracted with ether (2 × 10 mL). The organic layers were combined, dried with MgSO₄, and filtered. The solvent was removed by rotary evaporation yielding a red-orange material that was separated on a Chromatotron (eluent hexane with gradual addition of CH₂Cl₂) furnishing **28**, as an orange powder

Table 2. Crystallographic collection and refinement parameters for **15**, **20**, **23**, and **28**.

Compound	15	20	23	28
Empirical formula	C ₂₂ H ₃₆ O ₇ P ₂ MnBF ₄	C ₁₅ H ₂₁ O ₅ P ₂ F ₆ Mn	C ₁₈ H ₁₄ O ₃ MnBF ₄	C ₁₈ H ₁₃ O ₃ Mn
Formula weight	616.20	512.20	420.04	332.22
Temperature (K)	173(2)	173(2)	173(2)	173(2)
Wavelength (Å)	0.71073	0.71073	0.71073	0.71073
Crystal system	Triclinic	Orthorhombic	Monoclinic	Monoclinic
Space group	<i>P</i> $\bar{1}$	<i>Pnma</i>	<i>P2</i> ₁ / <i>n</i>	<i>C2</i>
<i>a</i> (Å)	9.3299(19)	15.694(5)	7.733(2)	25.577(14)
<i>b</i> (Å)	11.082(2)	10.991(4)	7.774(2)	6.255(3)
<i>c</i> (Å)	12.969(3)	11.735(4)	28.795(7)	9.362(5)
α (°)	97.600(3)	90	90	90
β (°)	94.229(3)	90	96.660(4)	107.230(8)
γ (°)	91.929(3)	90	90	90
Volume (Å ³)	1324.2(5)	2024.4(11)	1719.4(7)	1430.5(14)
<i>Z</i>	2	4	4	4
<i>D</i> _{calcd.} (Mg/m ³)	1.545	1.681	1.623	1.543
Absorption coefficient (mm ⁻¹)	0.688	0.889	0.825	0.932
<i>F</i> (000)	640	1040	848	680
Crystal size (mm)	0.18 × 0.42 × 0.44	0.32 × 0.45 × 0.70	0.12 × 0.28 × 0.42	0.03 × 0.05 × 0.50
Theta range for data collection (°)	1.59 to 27.52	2.17 to 27.69	1.42 to 27.50	1.67 to 27.51
Index ranges	-12 ≥ <i>h</i> ≥ 11 -14 ≥ <i>k</i> ≥ 14 -16 ≥ <i>l</i> ≥ 15	-20 ≥ <i>h</i> ≥ 18 -14 ≥ <i>k</i> ≥ 14 -14 ≥ <i>l</i> ≥ 15	-9 ≥ <i>h</i> ≥ 10 -9 ≥ <i>k</i> ≥ 10 -37 ≥ <i>l</i> ≥ 37	-32 ≥ <i>h</i> ≥ 32 -8 ≥ <i>k</i> ≥ 8 -12 ≥ <i>l</i> ≥ 11
Reflections collected	11 886	16 907	14 780	6 352
Independent reflections	5981 [<i>R</i> (int) = 0.0259]	2455 [<i>R</i> (int) = 0.0419]	3936 [<i>R</i> (int) = 0.0290]	2802 [<i>R</i> (int) = 0.0604]
Absorption correction	SADABS	SADABS	SADABS	SADABS
Refinement method	Full-matrix least-squares on <i>F</i> ²	Full-matrix least-squares on <i>F</i> ²	Full-matrix least-squares on <i>F</i> ²	Full-matrix least-squares on <i>F</i> ²
Data/restraints/parameters	5981/0/334	2452/0/222	3935/0/240	2802/0/200
Goodness-of-fit on <i>F</i> ²	1.047	1.164	1.051	1.034
Final <i>R</i> indices [<i>I</i> > 2σ(<i>I</i>)]	<i>R</i> 1 = 0.0368, <i>wR</i> 2 = 0.0938	<i>R</i> 1 = 0.0343, <i>wR</i> 2 = 0.0882	<i>R</i> 1 = 0.0481, <i>wR</i> 2 = 0.1208	<i>R</i> 1 = 0.0520, <i>wR</i> 2 = 0.0925
<i>R</i> indices (all data)	<i>R</i> 1 = 0.0455, <i>wR</i> 2 = 0.0988	<i>R</i> 1 = 0.0469, <i>wR</i> 2 = 0.0991	<i>R</i> 1 = 0.0588, <i>wR</i> 2 = 0.1272	<i>R</i> 1 = 0.0894, <i>wR</i> 2 = 0.1044
Extinction coefficient		0.0000(3)	0.0001(7)	0.0000(7)
Absolute structure parameter				0.50(3)
Largest diff. peak and hole (e ⁻ Å ⁻³)	0.423 and -0.358	0.538 and -0.712	1.033 and -1.215	0.412 and -0.372

(0.131 g, 0.395 mmol, 44%). IR (NaCl windows, CDCl₃, cm⁻¹) ν_{CO} : 2022 (s), 1950 (s). ¹H NMR (500 MHz, CD₂Cl₂) δ : 7.05 (m, 4H, aromatic CH), 5.61 (t, 1H, *J* = 5.1 Hz, CH), 5.18 (t, 1H, *J* = 6.3 Hz, CH), 5.09 (d, 1H, *J* = 5.3 Hz, CH), 4.41 (d, 1H, *J* = 7.3 Hz, CH), 4.10 (s, 1H, CH), 3.23 (m, 2H, CH₂), 2.47 (m, 2H, CH₂). ¹³C NMR (125 MHz, CD₂Cl₂) δ : 222.4 (Mn-CO), 138.7, 133.5, 130.1, 129.5, 126.6, 125.3, 106.7, 100.3, 98.6, 74.8, 74.6, 60.8, 38.0, 36.4, 32.9. MS (DEI, *m/z* (%)): 332 (2, [M]⁺), 276 (3.2, [M - 2CO]⁺), 248 (3.2, [M - 3CO]⁺), 193 (100, [C₁₅H₁₃]⁺). Anal. calcd. for C₁₈H₁₃MnO₃ (%): C 65.06, H 3.92; found: C 65.45, H 3.96. A rod-shaped, orange crystalline sample suit-

able for structural determination by single-crystal X-ray diffraction studies was grown from dichloromethane by slow evaporation under an atmosphere of nitrogen at room temperature.

X-ray crystal structure determinations³

X-ray crystallographic data (see Tables 1 and 2) were collected from single crystal samples, each of which was mounted on a glass fibre. Data were collected using a P4 Bruker diffractometer, equipped with a Bruker SMART 1K charge coupled device (CCD) area detector, using the program SMART (48), and a rotating anode, using graphite-

³Supplementary data for this article are available on the journal Web site (canjchem.nrc.ca) or may be purchased from the Depository of Unpublished Data, Document Delivery, CISTI, National Research Council Canada, Ottawa, ON K1A 0R6, Canada. DUD 3811. For more information on obtaining material refer to cisti-icist.nrc-cnrc.gc.ca/cms/unpub_e.shtml. CCDC 681235 (3), 681234 (4), 681228 (7), 681233 (8), 681232 (15), 681231 (20), 681230 (23), and 681229 (28) contain the crystallographic data for this manuscript. These data can be obtained, free of charge, via www.ccdc.cam.ac.uk/conts/retrieving.html (Or from the Cambridge Crystallographic Data Centre, 12 Union Road, Cambridge CB2 1EZ, UK; fax +44 1223 336033; or deposit@ccdc.cam.ac.uk).

monochromated Mo K α radiation ($\lambda = 0.71073 \text{ \AA}$). The crystal-to-detector distance was 4.987 cm, and the data collection was carried out in 512×512 pixel mode, utilizing 2×2 pixel binning. The initial unit cell parameters were determined by a least-squares fit of the angular settings of the strong reflections, collected by a 12° scan in 40 frames over three different sections of reciprocal space (160 frames in total). A hemisphere of data was collected with high redundancy, to better than 0.8 \AA resolution at 153 K. Upon completion of the data collection, the first 40 frames were recollected to improve the decay correction analyses. Processing was carried out using the program SAINT (49), which applied Lorentz and polarization corrections to the three-dimensionally integrated diffraction spots. The program SADABS (50), was utilized for the scaling of the diffraction data, the application of a decay correction, and an empirical absorption correction based on redundant reflections for the data set. The structures were solved by using the direct-methods procedure in the Bruker SHELXTL program library (51), and refined by full-matrix least-squares methods on F^2 with anisotropic thermal parameters for all nonhydrogen atoms. Hydrogen atoms were either found and added from the difference map, and allowed to refine isotropically, or were added as fixed contributors at calculated positions, with isotropic thermal parameters based on the carbon atom to which they were bonded.

The structure of **3** exhibited a disorder between one of the carbonyl groups and a bromine atom and hence, the occupancy of the two conformations was allowed to refine as a free variable (final ratio of approximately 70:30). Likewise, the final structure of **4** was based on a disorder model in which the $\text{Mn}(\text{CO})_2\text{I}$ tripod could exist in two conformations. The occupancy of the two conformations was allowed to refine as a free variable (final ratio of approximately 88:12). In the case of $[(\eta^6\text{-tetalin})\text{Mn}(\text{CO})_2\text{P}(\text{OMe})_3][\text{PF}_6]$ (**20**) the molecule lies on a crystallographic mirror plane; thus only half of the molecule was refined and the other half was generated by the mirror plane. This arises because of a disorder between C(7) and C(7a) such that there are two twisted half-chair conformations. Also, the anion was disordered, and two orientations were found for the PF_6 anion.³

Acknowledgements

Financial support from the Natural Sciences and Engineering Research Council of Canada (NSERC), from Science Foundation Ireland, and from University College Dublin, is gratefully acknowledged. Mass spectra were acquired courtesy of Dr. Kirk Green of the McMaster Regional Mass Spectrometry Facility. We also thank Dr. James F. Britten for X-ray crystallographic advice.

References

- (a) G. Mehta, S.R. Shah, and K. Ravikumar. *J. Chem. Soc. Chem. Commun.* 1006 (1993); (b) H. Sakurai, T. Daiko, and T. Hirao. *Science (Washington, D.C.)*, **301**, 1878 (2003).
- H.K. Gupta, P.E. Lock, and M.J. McGlinchey. *Organometallics*, **16**, 3628 (1997).
- H.K. Gupta, P.E. Lock, D.W. Hughes, and M.J. McGlinchey. *Organometallics*, **16**, 4355 (1997).
- (a) J.-R. Hamon, J.-Y. Saillard, A. Le Beuze, M.J. McGlinchey, and D. Astruc. *J. Am. Chem. Soc.* **104**, 7549 (1982); (b) C. Valério, E. Alonzo, J. Ruiz, J.-C. Blais, and D. Astruc. *Angew. Chem. Int. Ed. Engl.* **38**, 1747 (1999), and refs. cited therein.
- (a) D.M. LaBrush, D.P. Eyman, N.C. Baenziger, and L.M. Mallis. *Organometallics*, **10**, 1026 (1991); (b) J.L. Moler, D.P. Eyman, J.M. Neilson, A.M. Morken, S.J. Schauer, and D.B. Snyder. *Organometallics*, **12**, 3304 (1993).
- N. Reginato and M.J. McGlinchey. *Organometallics*, **20**, 4147 (2001).
- (a) S. Sun, C.A. Dullaghan, and D.A. Sweigart. *J. Chem. Soc. Dalton Trans.* 4493 (1996); (b) R.D. Pike and D.A. Sweigart. *Coord. Chem. Rev.* **187**, 183 (1999).
- G. Jaouen, S. Top, A. Laconi, D. Couturier, and J. Brossard. *J. Am. Chem. Soc.* **106**, 2207 (1984).
- D. Astruc. *Acc. Chem. Res.* **33**, 287 (2000), and refs. cited therein.
- H.-J. Choi, Y.S. Park, S.H. Yun, H.-S. Kim, C.S. Cho, K. Ko, and K.H. Ahn. *Org. Lett.* **4**, 795 (2002).
- (a) H.K. Gupta, S. Brydges, and M.J. McGlinchey. *Organometallics*, **18**, 115 (1999); (b) S. Brydges, L.E. Harrington, and M.J. McGlinchey. *Coord. Chem. Rev.* **233–234**, 75 (2002).
- R.J. Bernhardt, M.A. Wilmoth, J.J. Weers, D.M. LaBrush, D.P. Eyman, and J.C. Huffman. *Organometallics*, **5**, 883 (1986).
- L.H.P. Gommans, L. Main, and B.K. Nicholson. *J. Organomet. Chem.* **346**, 385 (1988).
- L.A.P. Kane-Maguire and D.A. Sweigart. *Inorg. Chem.* **18**, 700 (1979).
- R.J. Bernhardt and D.P. Eyman. *Organometallics*, **3**, 1445 (1984).
- P.J. Schlom, A.M. Morken, D.P. Eyman, N.C. Baenziger, and S.J. Schauer. *Organometallics*, **12**, 3461 (1993).
- (a) P.J.C. Walker and R.J. Mawby. *Inorg. Chim. Acta*, **7**, 621 (1973); (b) There is an early report of $t\text{-Bu-OCO-Co}(\text{CO})_4$: R.F. Heck. *J. Organomet. Chem.* **2**, 195 (1964).
- R.B. King. *J. Organomet. Chem.* **23**, 527 (1970).
- A. Decken, J.F. Britten, and M.J. McGlinchey. *J. Am. Chem. Soc.* **115**, 7275 (1993).
- R.H. Crabtree and C.P. Parnell. *Organometallics*, **3**, 1727 (1984).
- O.I. Trifonova, E.A. Ochertyanova, N.G. Akhmedov, V.A. Roznyatovsky, D.N. Laikov, N.A. Ustynyuk, and Y.A. Ustynyuk. *Inorg. Chim. Acta*, **280**, 328 (1998).
- F. Rose-Munch, C. Susanne, C. Renard, E. Rose, and J. Vaissermann. *J. Organomet. Chem.* **519**, 253 (1996).
- D.A. Brown, W.K. Glass, K.M. Kreddan, D. Cunningham, P.A. McArdle, and T. Higgins. *J. Organomet. Chem.* **418**, 91 (1991).
- D.B. Snyder, S.J. Schauer, D.P. Eyman, J.L. Moler, and J.J. Weers. *J. Am. Chem. Soc.* **115**, 6718 (1993).
- T.-Y. Lee, S.S. Lee, Y.K. Chung, and S.W. Lee. *J. Organomet. Chem.* **486**, 141 (1995).
- (a) K. Woo, G.B. Carpenter, and D.A. Sweigart. *Inorg. Chim. Acta*, **220**, 297 (1994); (b) K. Woo, P.G. Williard, D.A. Sweigart, N.W. Duffy, B.H. Robinson, and J. Simpson. *J. Organomet. Chem.* **487**, 111 (1995).
- T. Volk, D. Bernicke, J.W. Bats, and H.-G. Schmalz. *Eur. J. Inorg. Chem.* 1883 (1998).
- M.J. McGlinchey. *Adv. Organomet. Chem.* **34**, 285 (1992), and refs. cited therein.
- A. Cecccon, A. Gambaro, and A. Venzo. *J. Organomet. Chem.* **281**, 221 (1985).
- T. Whitesides and R. Budnik. *Inorg. Chem.* **15**, 874 (1976).

31. P.J.P. Reboul, B. Cristau, and G. Pèpe. *Acta Crystallogr.* **B37**, 394 (1981).
32. W. Weissensteiner, O. Hofer, and U.G. Wagner. *J. Org. Chem.* **53**, 3988 (1988).
33. (a) R.C. Cambie, G.R. Clark, A.C. Gourdie, P.S. Rutledge, and P.D. Woodgate. *J. Organomet. Chem.* **297**, 177 (1985); (b) B. Mailvaganam, R.E. Perrier, B.G. Sayer, B.E. McCarry, R.A. Bell, and M.J. McGlinchey. *J. Organomet. Chem.* **354**, 325 (1988).
34. R.M. Moriarty, Y.-Y. Ku, U.S. Gill, R. Gilardi, R.E. Perrier, and M.J. McGlinchey. *Organometallics*, **8**, 960 (1989).
35. A. Vessières, S. Top, A.A. Ismail, I.S. Butler, M. Louer, and G. Jaouen. *Biochemistry*, **27**, 6659 (1988).
36. W.A. Herrmann, J. Plank, G.W. Kriechbaum, M.L. Ziegler, H. Pfisterer, J.L. Atwood, and R.D. Rogers. *J. Organomet. Chem.* **264**, 327 (1984).
37. M.R. Churchill and S. Scholer. *Inorg. Chem.* **8**, 1950 (1969).
38. J.M. Veauthier, A. Chow, G. Fraenkel, S.J. Geib, and N.J. Cooper. *Organometallics*, **19**, 3942 (2000).
39. J.M. Veauthier, A. Chow, G. Fraenkel, S.J. Geib, and N.J. Cooper. *Organometallics*, **19**, 661 (2000).
40. (a) P.M. Treichel and J.W. Johnson. *Inorg. Chem.* **16**, 749 (1977); (b) P.M. Treichel, K.P. Fivizzani, and K.J. Haller. *Organometallics*, **1**, 931 (1982).
41. (a) J.W. Johnson and P.M. Treichel. *J. Chem. Soc. Chem. Commun.* 688 (1976); (b) J.W. Johnson and P.M. Treichel. *J. Am. Chem. Soc.* **99**, 1427 (1977); (c) E. Kirillov, S. Kahlal, T. Roisnel, T. Georgelin, J.-Y. Saillard, and J.-F. Carpentier. *Organometallics*, **27**, 387 (2008).
42. A. Xia, J.P. Selegue, A. Carrilo, and C.P. Brock. *J. Am. Chem. Soc.* **122**, 3973 (2000).
43. S. Brydges, N. Reginato, L.P. Cuffe, C.M. Seward, and M.J. McGlinchey. *C. R. Chim.* **8**, 1497 (2005).
44. M. Brookhart and M.L.H. Green. *J. Organomet. Chem.* **250**, 395 (1983).
45. E. Folga and T. Zeigler. *J. Am. Chem. Soc.* **115**, 5169 (1993).
46. J.K. Klassen, M. Selke, A.A. Sorensen, and G.K. Yang. *J. Am. Chem. Soc.* **112**, 1267 (1990).
47. L.D. Hicks, J.K. Han, and A.J. Fry. *Tetrahedron Lett.* **41**, 7817 (2000).
48. Bruker AXS, Inc. SMART. Release 5.611 [computer program]. Bruker AXS, Inc., Madison, Wis. 2000.
49. Bruker AXS, Inc. SAINT. Release 6.02a [computer program]. Bruker AXS, Inc., Madison, Wis. 2000.
50. G.M. Sheldrick. SADABS [computer program]. Bruker AXS Inc., Madison, Wis. 2000.
51. G.M. Sheldrick. SHELXTL. Version 5.1 [computer program]. Bruker AXS, Inc., Madison, Wis. 1998.